













# Mitochondrial dysfunction in human hypertrophic cardiomyopathy is linked to cardiomyocyte architecture disruption and corrected by improving NADH-driven mitochondrial respiration

Edgar E. Nollet <sup>1,2</sup>, Inez Duursma <sup>1,2</sup>, Anastasiya Rozenbaum<sup>1,2</sup>,  
Moritz Eggelbusch <sup>3,4,5</sup>, Rob C.I. Wüst <sup>3</sup>, Stephan A.C. Schoonvelde <sup>6</sup>,  
Michelle Michels <sup>6</sup>, Mark Jansen <sup>7</sup>, Nicole N. van der Wel <sup>8</sup>,  
Kenneth C. Bedi Jr <sup>9</sup>, Kenneth B. Margulies <sup>9</sup>, Jeff Nirschl<sup>10</sup>,  
Diederik W.D. Kuster <sup>1,2</sup>, and Jolanda van der Velden <sup>1,2\*</sup>

<sup>1</sup>Department of Physiology, Amsterdam UMC, Location VUmc, O2 Science building—11W53, De Boelelaan 1108, 1081HZ Amsterdam, The Netherlands; <sup>2</sup>Amsterdam Cardiovascular Sciences, Heart failure & Arrhythmias, Amsterdam UMC, Location VUmc, O2 Science building, De Boelelaan 1108, 1081 HZ Amsterdam, The Netherlands; <sup>3</sup>Laboratory for Myology, Faculty of Behavioural and Movement Sciences, Amsterdam Movement Sciences, Vrije Universiteit Amsterdam, Amsterdam, The Netherlands; <sup>4</sup>Department of Nutrition and Dietetics, Amsterdam UMC, Amsterdam, The Netherlands; <sup>5</sup>Faculty of Sports and Nutrition, Center of Expertise Urban Vitality, Amsterdam University of Applied Sciences, Amsterdam, The Netherlands; <sup>6</sup>Department of Cardiology, Erasmus MC, Rotterdam, The Netherlands; <sup>7</sup>Division of Genetics, UMC Utrecht, Utrecht, The Netherlands; <sup>8</sup>Department of Medical Biology, Electron Microscopy Centre, Amsterdam UMC, Amsterdam, The Netherlands; <sup>9</sup>Cardiovascular Institute, Perelman School of Medicine, Philadelphia, PA, USA; and <sup>10</sup>Department of Pathology, Stanford University, Stanford, USA

Received 11 June 2022; revised 19 December 2022; accepted 12 January 2023; online publish-ahead-of-print 3 February 2023

See the editorial comment for this article ‘Targeting mitochondria in hypertrophic cardiomyopathy’, by Vasco Sequeira et al., <https://doi.org/10.1093/eurheartj/ehad081>.

## Abstract

### Aims

Genetic hypertrophic cardiomyopathy (HCM) is caused by mutations in sarcomere protein-encoding genes (i.e. genotype-positive HCM). In an increasing number of patients, HCM occurs in the absence of a mutation (i.e. genotype-negative HCM). Mitochondrial dysfunction is thought to be a key driver of pathological remodelling in HCM. Reports of mitochondrial respiratory function and specific disease-modifying treatment options in patients with HCM are scarce.

### Methods and results

Respirometry was performed on septal myectomy tissue from patients with HCM ( $n = 59$ ) to evaluate oxidative phosphorylation and fatty acid oxidation. Mitochondrial dysfunction was most notably reflected by impaired NADH-linked respiration. In genotype-negative patients, but not genotype-positive patients, NADH-linked respiration was markedly depressed in patients with an indexed septal thickness  $\geq 10$  compared with  $< 10$ . Mitochondrial dysfunction was not explained by reduced abundance or fragmentation of mitochondria, as evaluated by transmission electron microscopy. Rather, improper organization of mitochondria relative to myofibrils (expressed as a percentage of disorganized mitochondria) was strongly associated with mitochondrial dysfunction. Pre-incubation with the cardiolipin-stabilizing drug elamipretide and raising mitochondrial  $\text{NAD}^+$  levels both boosted NADH-linked respiration.

### Conclusion

Mitochondrial dysfunction is explained by cardiomyocyte architecture disruption and is linked to septal hypertrophy in genotype-negative HCM. Despite severe myocardial remodelling mitochondria were responsive to treatments aimed at restoring respiratory function, eliciting the mitochondria as a drug target to prevent and ameliorate cardiac disease in HCM. Mitochondria-targeting therapy may particularly benefit genotype-negative patients with HCM, given the tight link between mitochondrial impairment and septal thickening in this subpopulation.

\* Corresponding author. Tel: + 31 (0)20 4448111. Email: [j.vandervelden1@amsterdamumc.nl](mailto:j.vandervelden1@amsterdamumc.nl)

© The Author(s) 2023. Published by Oxford University Press on behalf of the European Society of Cardiology.

This is an Open Access article distributed under the terms of the Creative Commons Attribution-NonCommercial License (<https://creativecommons.org/licenses/by-nc/4.0/>), which permits non-commercial re-use, distribution, and reproduction in any medium, provided the original work is properly cited. For commercial re-use, please contact [journals.permissions@oup.com](mailto:journals.permissions@oup.com)

## Structured Graphical Abstract

### Key Question

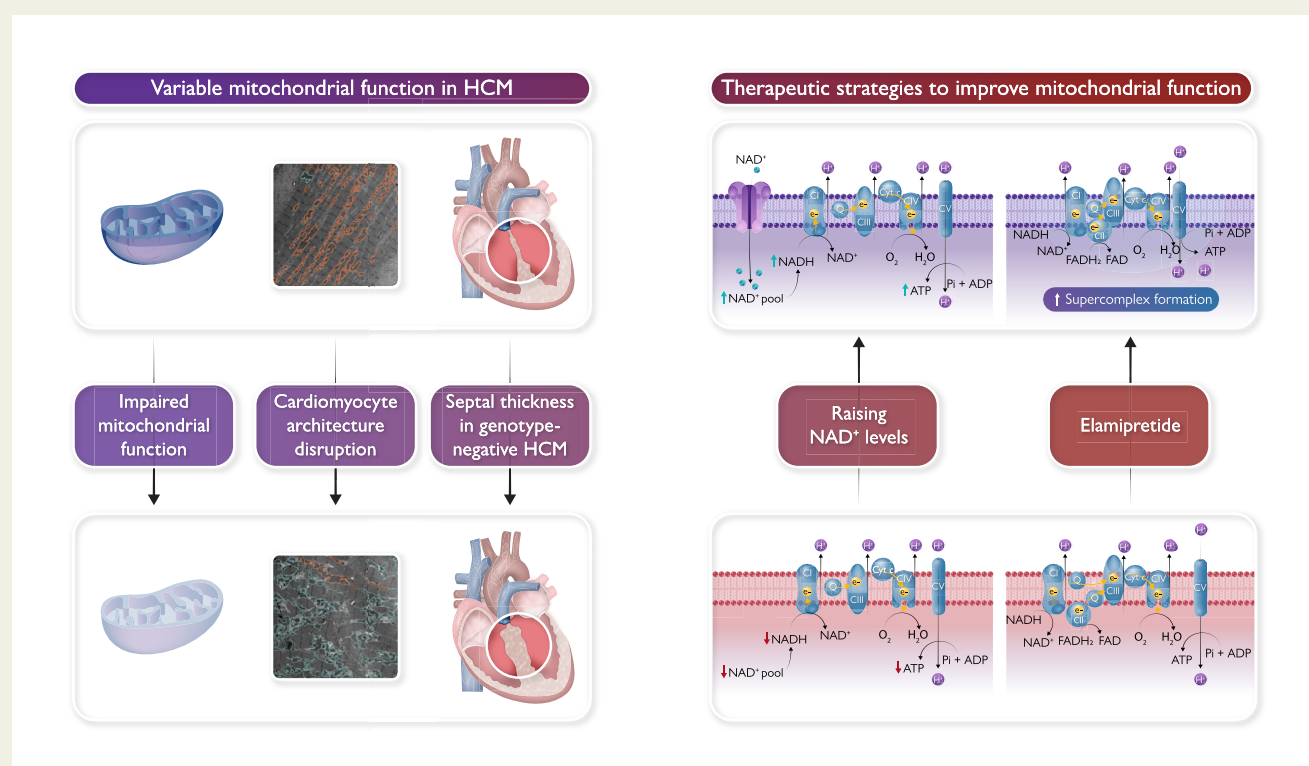
Mitochondrial dysfunction may be a key driver of disease in patients with hypertrophic cardiomyopathy (HCM). Comprehensive reports on alterations of mitochondrial function in human subjects are lacking, in particular in genotype-negative patients.

### Key Finding

In genotype-negative patients, but not genotype-positive patients, mitochondrial dysfunction was linked to septal hypertrophy. Ultrastructural analyses revealed a tight link between disruption of cardiomyocyte architecture and mitochondrial dysfunction. Treatment with NAD<sup>+</sup> and elamipretide both boosted mitochondrial respiration by improving NADH-driven respiration.

### Take Home Message

Mitochondrial dysfunction is explained by disruption of cardiomyocyte architecture and is linked to septal hypertrophy in genotype-negative HCM. Therapies aimed at improving mitochondrial performance may prevent or improve cardiac disease in HCM, particularly in genotype-negative patients.



Our analyses reveal substantial variation in mitochondrial dysfunction in patients with hypertrophic cardiomyopathy. At the cellular level, this was strongly linked to mitochondrial disorganization. In patients with no known causative sarcomere mutation, mitochondrial dysfunction was associated with septal thickening. Mitochondria were responsive to treatments aimed at boosting NADH-driven respiration, indicating therapeutic potential of the mitochondria despite severe cardiac remodelling.

### Keywords

Hypertrophic cardiomyopathy • Mitochondrial dysfunction • Metabolism • Cardiomyocyte architecture • Mitochondrial therapy

## Translational perspective

Hypertrophic cardiomyopathy is a highly prevalent cardiac disease and may be driven by mitochondrial dysfunction. We show a strong link between disease severity and mitochondrial dysfunction in patients with no causative mutation. Mitochondrial dysfunction was corrected by stimulating NADH-driven respiration, indicating therapeutic potential despite advanced disease. The majority of newly diagnosed patients carry no causative mutation and may be less responsive to myofilament-targeting therapies. These patients may, therefore, particularly benefit from mitochondrial therapy. At the cellular level, mitochondrial dysfunction was strongly associated with mitochondrial disorganization, implying maintenance of cardiomyocyte architecture as an important research area in cardiac disease.

## Introduction

Hypertrophic cardiomyopathy (HCM) is a highly common inherited cardiomyopathy,<sup>1</sup> characterized by impaired diastolic function and asymmetrical hypertrophy of the left ventricle (LV), frequently resulting in LV outflow tract (LVOT) obstruction.<sup>2,3</sup> Patients frequently carry a heterozygous causative mutation in sarcomere protein-encoding genes (termed genotype-positive;  $G_{\text{positive}}$ ). An increasing number of patients, however, do not carry a mutation (termed genotype-negative;  $G_{\text{negative}}$ ).<sup>4–6</sup> In  $G_{\text{negative}}$  patients, the underlying aetiology of the disease is largely unclear.

Metabolic perturbations and energetic impairment represent major pathological features in manifest HCM. At the cellular level, this has been linked to mutation-driven inefficient sarcomere performance with increased ATP utilization,<sup>7–11</sup> leading to a chronic increase in cardiac workload and energetic stress.<sup>12</sup> In imaging studies in both  $G_{\text{positive}}$  and  $G_{\text{negative}}$  patients, cardiac inefficiency and energetic impairment are apparent from a reduced phosphocreatine/ATP ratio and lower myocardial external efficiency (MEE) compared with healthy individuals.<sup>9,13–15</sup> Thus, in  $G_{\text{negative}}$  patients, metabolic perturbations may be linked to remodelling-induced homeostatic disturbances. In line with imaging studies, recent multi-omics analyses in myectomy tissue from patients with HCM revealed perturbations in oxidative mitochondrial metabolism, suggesting impaired mitochondrial respiratory function.<sup>16,17</sup> However, comprehensive studies of mitochondrial respiratory function have exclusively been conducted in animal models of HCM.<sup>18,19</sup> Reduced MEE is already observed in sarcomere mutation carriers without hypertrophy, indicating metabolic alterations occur at an early disease stage.<sup>9,15</sup> Counteracting metabolic stress by preventing or ameliorating mitochondrial dysfunction may, therefore, represent a treatment strategy to halt or reverse disease development. Current (pharmacological) treatment options in patients with HCM are invasive or not disease-specific and are aimed at symptom relief,<sup>20</sup> underscoring the need for early-disease treatment options. The aim of this study was to gain insight into impaired mitochondrial respiratory function and identify therapeutic potential in human HCM.

To this end, we performed mitochondrial respirometry measurements and ultrastructural tissue analysis in a large amount of myectomy samples from a clinically well-characterized cohort of patients with LVOT obstruction. Mitochondrial respiratory failure varied strikingly and was correlated with septal hypertrophy in  $G_{\text{negative}}$ , but not  $G_{\text{positive}}$  patients. The severity of mitochondrial dysfunction was significantly associated with improper mitochondrial organization relative to myofibrils. Mitochondrial respiratory function could be improved *ex vivo* (i) via incubation with the cardiolipin-stabilizing drug elamipretide<sup>21</sup> and (ii) by increasing mitochondrial nicotinamide adenine dinucleotide ( $\text{NAD}^+$ ) levels, suggesting targeting mitochondrial bioenergetics holds therapeutic potential despite severe cardiac remodelling in HCM myocardium.

## Methods

An extended methods section is provided in the [supplementary files](#).

### Human myocardial samples

Interventricular septal tissue of 59 consecutive patients with HCM was acquired during myectomy surgery to relieve LVOT obstruction (36 males and 23 females). Forty-seven patients underwent genetic testing as previously described,<sup>22</sup> 12 patients declined. A causative mutation was found in 23 patients (i.e.  $G_{\text{positive}}$ ); the other 24 patients were classified  $G_{\text{negative}}$

([Figure 1](#)). Left ventricle free wall (mid-ventricle) tissue samples from 14 non-failing donors with no history of cardiac disease were procured in accordance with protocols and ethical regulations approved by Institutional Review Boards at the University of Pennsylvania and the Gift-of-Life Donor Program (PA, USA). Hearts from non-failing donors were obtained during organ donation from brain-dead donors. All hearts were arrested *in situ* using ice-cold cardioplegia solution and kept on ice until flash-freezing in liquid nitrogen or fixation within 4 h of explantation as previously described.<sup>23</sup> Clinical and cardiac parameters of patients and donors are described in [Table 1](#). An overview of all techniques that were used and sample sizes per analysis are depicted in [Figure 1](#). [Supplementary material online, Table S1](#) describes individual information of each patient and donor, including which samples were used for each analysis.

## Mitochondrial respiratory function

### Sample preparation

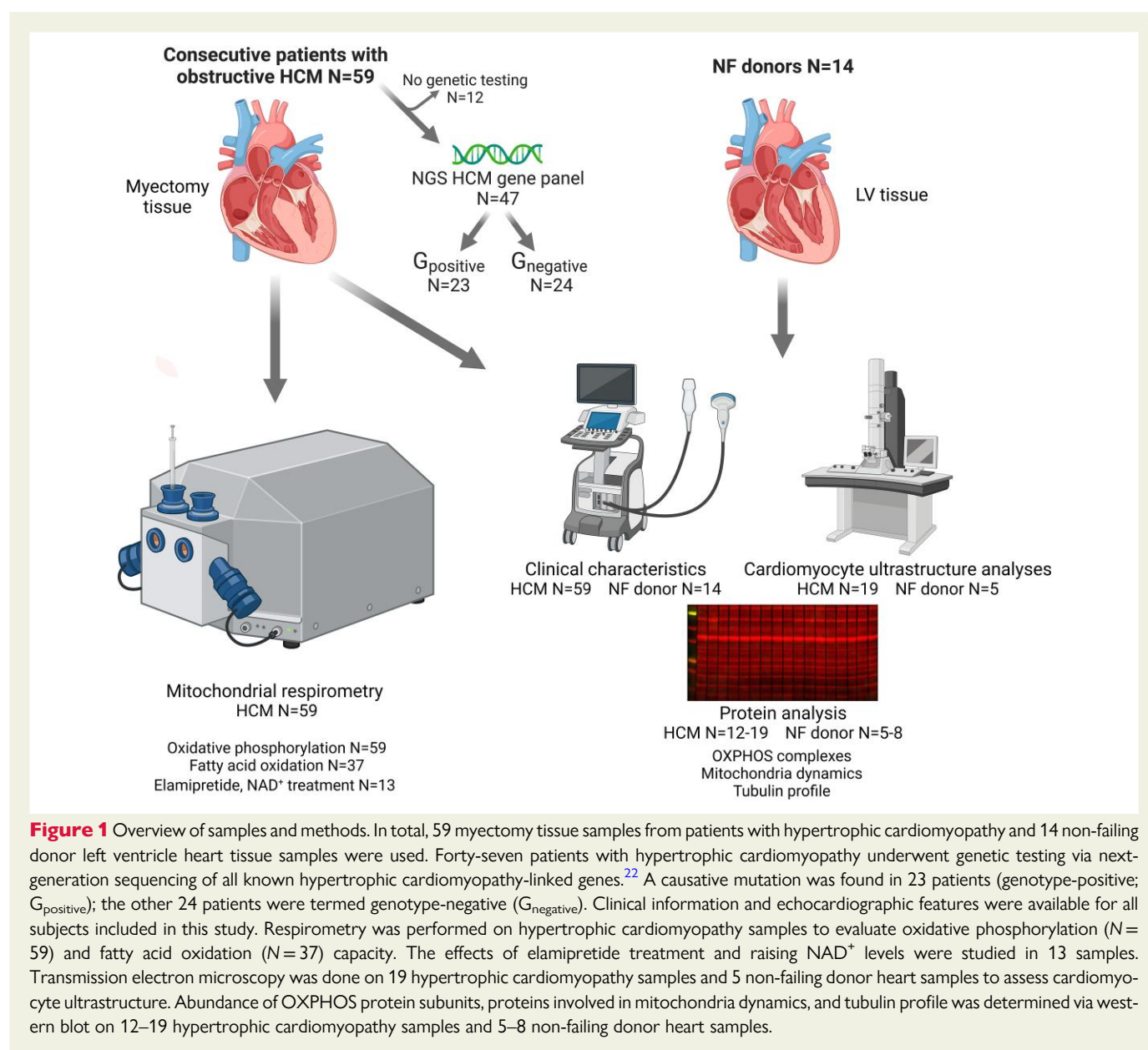
Respirometry was performed using small saponin-permeabilized bundles of fresh myectomy tissue. A detailed description of sample preparation is provided in the [supplementary files](#).

### Oxidative phosphorylation pathways

Leak respiration was evaluated using 10 mM sodium glutamate, 2 mM sodium malate, and 5 mM sodium pyruvate, providing electron input through NADH and complex I. Maximal NADH-linked respiration was measured after addition of 5 mM ADP. Cytochrome-c (10  $\mu\text{M}$ ) was added to assess outer mitochondrial membrane integrity. Maximal OXPHOS capacity, with simultaneous electron input through complexes I and II, was determined after adding 10 mM succinate. Excess capacity of the electron transferring complexes (I–IV) was measured through titration with a protonophore (carbonyl cyanide-*p*-trifluoromethoxyphenylhydrazone; FCCP) in 0.05  $\mu\text{M}$  steps. Succinate-linked respiration through complex II was evaluated after blocking complex I with 0.5  $\mu\text{M}$  rotenone. Antimycin-A (2.5  $\mu\text{M}$ ) was added to fully inhibit mitochondrial oxygen consumption and measure residual oxygen consumption, which was subtracted from all values as background. An overview of this respirometry protocol is depicted in [Figure 2A](#). In a subset of samples ( $n = 13$ ), the effect of the cardiolipin-stabilizing compound elamipretide on respiratory function was tested. Analogous to previous reports,<sup>24</sup> we incubated tissue fibres for 1 h in a preservation solution containing 100  $\mu\text{M}$  elamipretide (or an equivalent amount of  $\text{H}_2\text{O}$  as vehicle). Subsequent tissue fibre preparation and measurement procedures were carried out in the presence of 100  $\mu\text{M}$  elamipretide. Respirometry measurements were performed *in duplo* and values per sample were averaged. To analyse supercomplex composition, fresh myectomy tissue portions ( $n = 5$ ) were incubated with 100  $\mu\text{M}$  elamipretide (or  $\text{H}_2\text{O}$  as vehicle) for 1 h in preservation solution, snap-frozen in liquid nitrogen, and analysed via Blue Native gel electrophoresis,<sup>25</sup> described in the [supplementary files](#).

### Fatty acid oxidation

To evaluate functional changes in fatty acid oxidation in HCM, we measured mitochondrial octanoylcarnitine oxidation, which proceeds independently of the mitochondrial carnitine shuttle,<sup>26</sup> in a subset of samples ( $n = 37$ ). Before adding fatty acid as substrate, a low concentration of malate (0.1 mM) and ADP (5 mM) were added. Malate is converted by malate dehydrogenase to oxaloacetate which is needed for condensation with  $\beta$ -oxidation-derived acetyl-CoA into citrate, which is needed to prevent accumulation of acetyl-CoA and consequent inhibition of  $\beta$ -oxidation.<sup>27</sup> Next, octanoylcarnitine (0.2 mM) and cytochrome-c (10  $\mu\text{M}$ ) were added. The subsequent increase in respiration was taken as a value for fatty acid oxidation capacity. An overview of this protocol is shown in [Figure 3A](#). All measurements were performed *in duplo* and values per sample were averaged.



## Transmission electron microscopy

### Analyses of myofibrils and mitochondria

Myofibrillar area and mitochondrial area were quantified in 6 images of representative myocytes (6800–11 000× magnification) per sample using QuPath software and averaged. Mitochondrial morphology was determined in 6 images (9300–23 000× magnification) per sample and averaged. Organization of interfibrillar (IF) mitochondria was determined in 4800× magnification images. Mitochondria were first segmented automatically using a neural network (described in detail in the [supplementary files](#)). Images were annotated using QuPath software, in which all IF mitochondria were annotated as being normally organized or disorganized. Mitochondria were considered to be normally organized if they were aligned parallel to myofibrils. Mitochondria that appeared as clustered were considered to be normally organized if such clusters clearly originated from converging lanes of normally organized mitochondria. Accordingly, mitochondria that did not display alignment to sarcomeric structures or appeared as isolated clusters were annotated as disorganized. An overview of all processing steps is provided in the [Supplementary material online, Figure S5](#).

Examples of annotated images are shown in the [Supplementary material online, Figure S6](#). Annotations were performed blinded to sample ID. Percentages were calculated in 6–10 images per sample and averaged.

## Statistical analyses

Statistical analyses were performed using GraphPad Prism v9 software. Data were statistically analysed using an unpaired Student's *t*-test when comparing 2 groups or one-way analysis of variance (ANOVA) with Tukey's multiple comparisons test when comparing >2 groups. Data with significantly different standard deviations between groups (according to *F*-test when comparing 2 groups or the Brown–Forsythe test when comparing >2 groups) were analysed with Welch's *t*-test when comparing 2 groups or Brown–Forsythe ANOVA with Dunnett's T3 multiple comparisons test when comparing >2 groups. Data that did not pass normality testing (D'Agostino & Pearson) were analysed non-parametrically with the Mann–Whitney test when comparing 2 groups or the Kruskal–Wallis test with Dunn's multiple comparisons test when comparing >2 groups. Paired two-tailed *t*-tests were performed on data describing the



**Table 1** Clinical characteristics of non-failing donors and patients with hypertrophic cardiomyopathy

	NF donor (n = 14)	HCM all patients (n = 59)	P-value
Sex, male	50% (7)	61% (36)	0.55
Age, years	51 ± 19	53 ± 16	0.77
BMI (kg/m <sup>2</sup> )	25.7 ± 6.4	27.3 ± 4.1	0.36
	HCM G <sub>positive</sub> (n = 23)	HCM G <sub>negative</sub> (n = 24)	P-value
Sex, male	61% (14)	67% (16)	0.77
Age, years	46 ± 16	56 ± 16	0.02*
BMI (kg/m <sup>2</sup> )	26.6 ± 4.0	27.5 ± 4.2	0.47
<b>Dimensions</b>			
IVSi	11.4 ± 3.4	10.3 ± 3.2	0.21
LADi	24.0 ± 4.2	24.2 ± 3.7	0.85
<b>Diastolic parameters</b>			
E/A	1.38 ± 0.85	1.21 ± 0.48	>0.99
E/e'	17.3 ± 6.9	19.1 ± 6.1	0.38
Deceleration time (ms)	244 ± 69	256 ± 80	0.86
<b>Diastolic dysfunction grade</b>			
1	30% (6)	24% (5)	0.73
≥2	70% (14)	76% (16)	
<b>Obstruction parameters</b>			
Rest LVOTg (mmHg)	52.3 ± 37.6	73.3 ± 41.1	0.09
Provoked LVOTg (mmHg)	65.4 ± 25.0	91.9 ± 29.5	0.01*
<b>Medication</b>			
β-blocker	76% (16)	63% (15)	0.76
Calcium channel blocker	24% (5)	29% (7)	0.74
Statins	14% (3)	21% (5)	0.70

Displayed are the mean ± standard deviation.

BMI, body mass index; IVSi, interventricular septum thickness normalized to body surface area; LADi, left atrial diameter normalized to body surface area; LVOTg, left ventricular outflow tract gradient; G<sub>negative</sub>, genotype-negative; G<sub>positive</sub>, genotype-positive.

\*P < 0.05.

## Results

### Variation in mitochondrial function is not explained by sarcomere mutation status or sex

We performed respirometry measurements in 59 myectomy samples from patients with HCM to characterize mitochondrial respiratory function in a clinically well-characterized population (Table 1 and see [Supplementary material online, Table S1](#)). Echocardiographic parameters were evaluated as previously described.<sup>28</sup> All patients with HCM displayed LVOT obstruction and varying degrees of diastolic impairment, apparent from an E/e' ratio >14, abnormally high LV filling pressure and/or left atrial dilation.<sup>29,30</sup> G<sub>negative</sub> patients were older at the time of myectomy and had worse provokable LVOT obstruction than G<sub>positive</sub> patients. Septal hypertrophy normalized to body surface area (IVSi) and diastolic function parameters were comparable for both patient groups. We applied two separate protocols (Figures 2A and 3A) to assess the functioning of OXPHOS pathways (i.e. leak respiration, NADH-linked respiration, total OXPHOS respiration, uncoupled respiration, and succinate-linked respiration) and mitochondrial fatty acid β-oxidation capacity. For all parameters that were acquired from these protocols, we observed remarkable interpatient variation (Figures 2C–J and 3C). We did not identify any significant differences between the average values of G<sub>positive</sub> and G<sub>negative</sub> patient groups. No sex differences were observed.

### Mitochondrial dysfunction is associated with septal hypertrophy in G<sub>negative</sub>, but not in G<sub>positive</sub> patients with hypertrophic cardiomyopathy

Measuring a large amount of patient samples enabled us to explore associations between mitochondrial function parameters and clinical and echocardiographic parameters (Figure 4). Age and body mass index (BMI) were not correlated to any mitochondrial function parameter. Significant negative associations were observed between IVSi and mitochondrial function parameters, most notably fatty acid oxidation capacity. NADH-linked respiration, uncoupled respiration, and NADH-linked respiration expressed as a fraction of total OXPHOS capacity were also negatively associated with IVSi, whereas succinate-linked respiration expressed as a fraction of uncoupled respiration was positively associated with IVSi (Figure 4A). Thus, as mitochondrial dysfunction progresses, NADH-linked respiration makes up a smaller proportion of total OXPHOS flux, whereas the relative contribution of succinate-linked respiration to total respiratory capacity increases. This suggests that worsening of mitochondrial dysfunction associated with septal growth is characterized by impairment of predominantly NADH-linked respiration. In line with this, we found a positive association between OXPHOS capacity and normalized NADH-linked respiration and a negative association between OXPHOS and normalized succinate-linked respiration.

While the clinical phenotype is similar, the underlying aetiology of the disease differs between G<sub>positive</sub> and G<sub>negative</sub> patients. We, therefore, assessed whether these patient groups displayed distinct associations between mitochondrial function and clinical phenotype (Figure 4B and C). Intriguingly, associations between IVSi and impaired mitochondrial function were absent in G<sub>positive</sub> patients (Figure 4B). In contrast, in G<sub>negative</sub> patients, IVSi correlated significantly with all but one

effect of treatments. Categorical distributions are presented as percentages and were analysed via Fisher's exact test. A two-tailed P < 0.05 was considered statistically significant. In case a Bonferroni multiple testing correction was applied, this is indicated in the figure legend. Correlations were tested via linear regression, in which case the coefficient of determination (R<sup>2</sup>) is reported, or described by Pearson's r. Data are displayed as mean ± standard error of the mean.

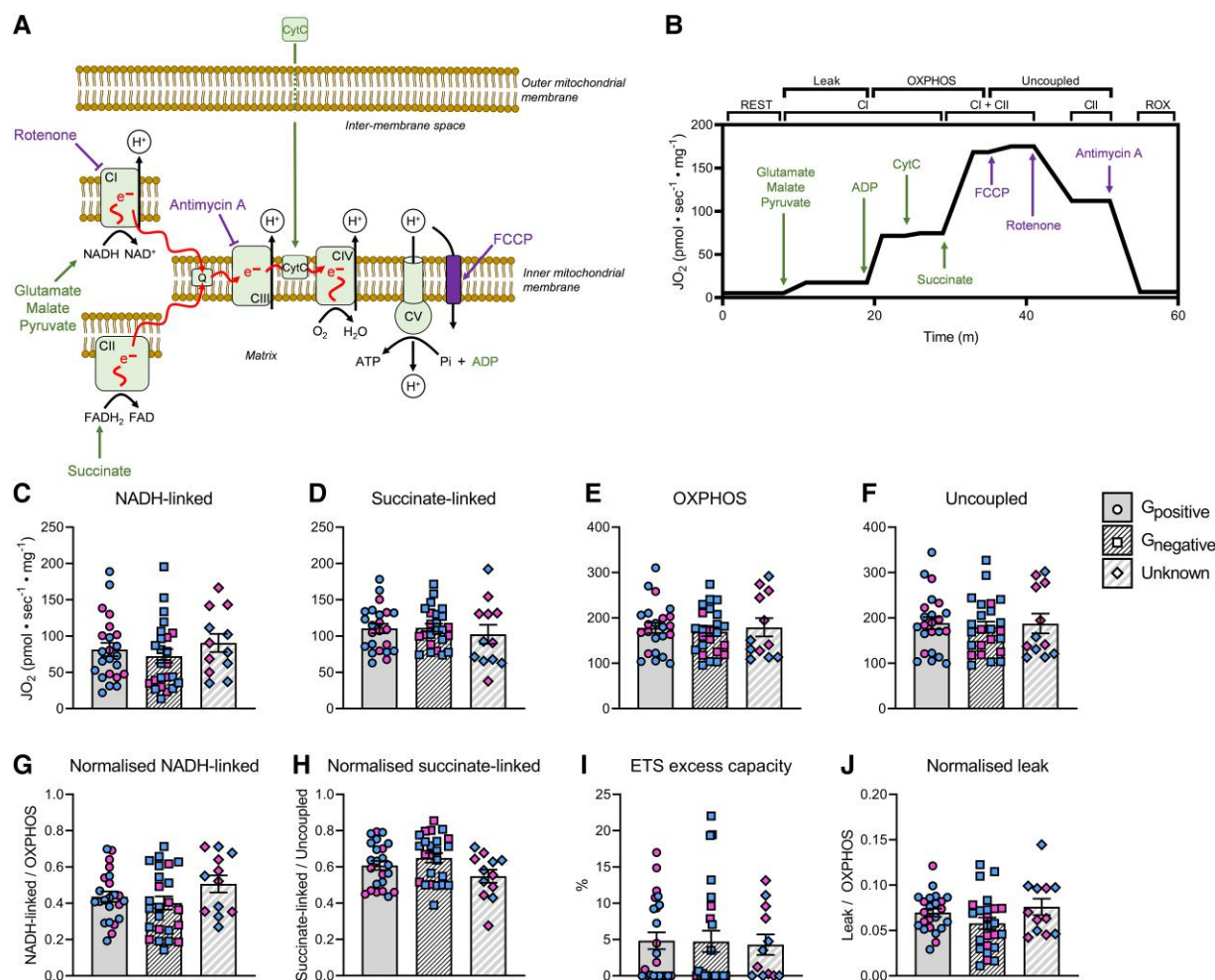
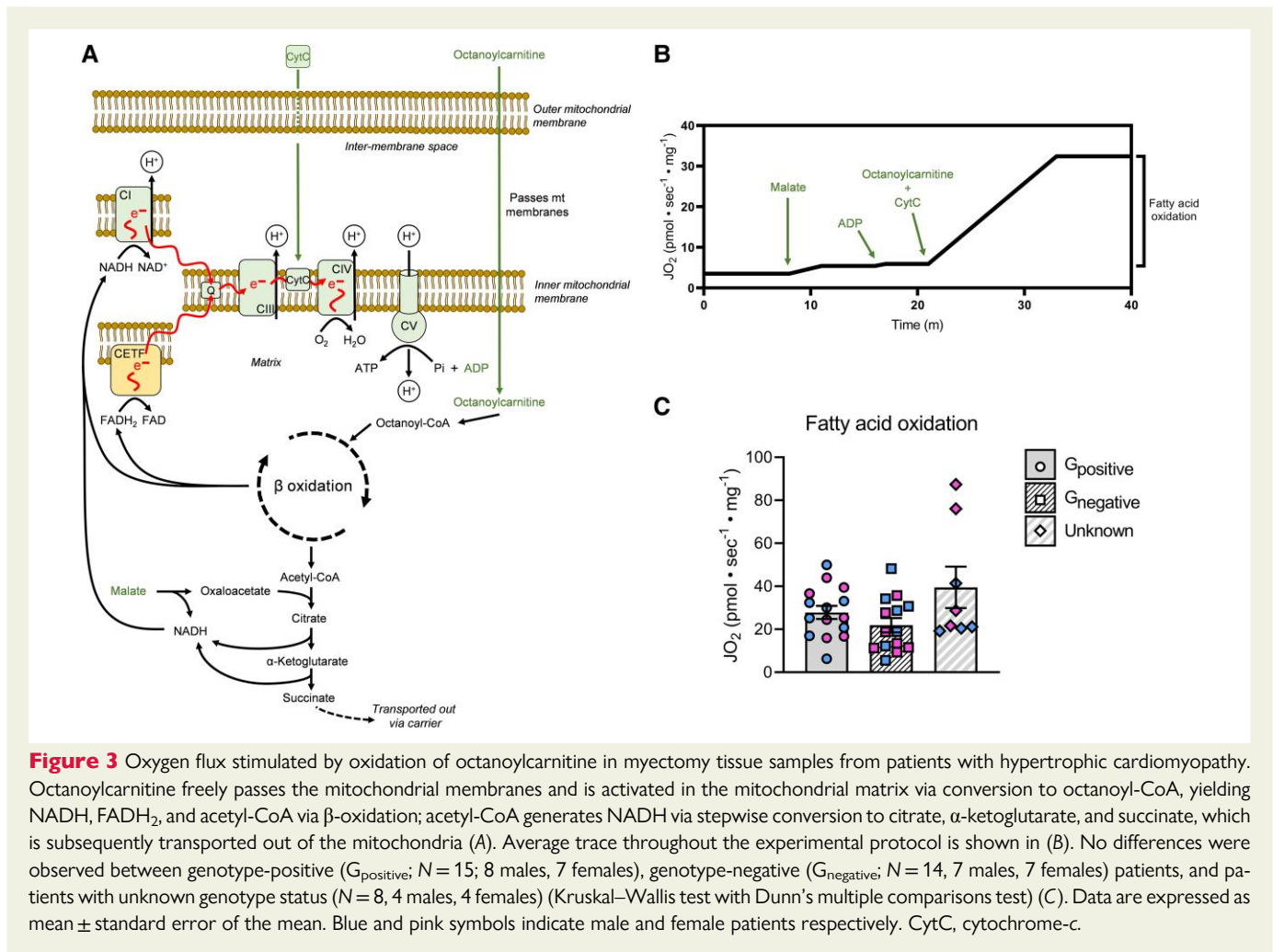


**Figure 2** Oxygen flux through oxidative phosphorylation (OXPHOS) pathways in myectomy tissue samples from patients with hypertrophic cardiomyopathy. The combination of substrates (green) and uncouplers/inhibitors (purple) that were used to evaluate respiration is shown in (A). Average trace throughout the experimental protocol and respiratory state of each combination of substrates, uncouplers, and inhibitors is shown in (B). Parameters in (C–F) are absolute values. Normalized NADH-linked respiration indicates NADH-linked respiration expressed as a fraction of OXPHOS capacity (G). Normalized succinate-linked respiration indicates succinate-linked respiration expressed as a fraction of uncoupled respiration (H). Electron transfer system excess capacity indicates the percentage difference between OXPHOS capacity and uncoupled respiration (I). Normalized leak indicates leak respiration expressed as a fraction of OXPHOS capacity (J). In all parameters that were acquired, no differences were observed between genotype-positive ( $G_{\text{positive}}$ ) patients ( $N = 23$ , 14 males, 9 females), genotype-negative ( $G_{\text{negative}}$ ) patients ( $N = 24$ , 16 males, 8 females), and patients with unknown genotype status ( $N = 12$ ; 6 males, 6 females) (C–J). Data are expressed as mean  $\pm$  standard error of the mean. Statistical tests: one-way analysis of variance with Tukey's multiple comparisons test in (C, D, F, and J); Brown–Forsythe analysis of variance with Dunnett's T3 multiple comparisons test in (E); the Kruskal–Wallis test with Dunn's multiple comparisons test in (G–I). Blue and pink symbols indicate male and female patients, respectively. CytC, cytochrome-c; FCCP, carbonyl cyanide *p*-trifluoro-methoxyphenyl hydrazone; ROX, residual oxygen consumption.

mitochondrial respiratory parameter (Figure 4C). These findings indicate that the interplay between mitochondrial dysfunction and septal growth is different in  $G_{\text{negative}}$  compared with  $G_{\text{positive}}$  HCM. Associations observed in  $G_{\text{negative}}$  patients between IVSi and mitochondrial function did not appear to be linearly correlated over the range of IVSi values (see Supplementary material online, Figure S1). Rather, respiratory parameters were significantly lower in samples from patients with an IVSi  $\geq 10$  compared with IVSi  $< 10$  samples. Therefore, we compared in both  $G_{\text{positive}}$  and  $G_{\text{negative}}$  patients, mitochondrial

parameters between patients with an IVSi  $\geq 10$  and patients with an IVSi  $< 10$  (Figure 5). In  $G_{\text{negative}}$  patients with an IVSi  $\geq 10$ , NADH-linked respiration, OXPHOS capacity, uncoupled respiration, normalized NADH-linked respiration, excess capacity of electron transferring complexes (I–IV), and fatty acid oxidation were lower and normalized succinate-linked respiration was higher compared with IVSi  $< 10$  (Figure 5J–R). In  $G_{\text{positive}}$  patients, fatty acid oxidation capacity was lower in IVSi  $\geq 10$  vs. IVSi  $< 10$  but no differences in other mitochondrial parameters were observed (Figure 5A–I).



## Mitochondrial dysfunction is not explained by myofibrillar and mitochondrial density or mitochondrial fragmentation

We performed TEM on a subset of samples ( $n = 19$ ) to assess whether mitochondrial dysfunction in HCM is associated with changes in cardiomyocyte ultrastructure (Figure 6). Myofibrillar area and mitochondrial area were unchanged in patients with HCM vs. non-failing donors, and among patients with HCM, there were no differences between  $G_{\text{negative}}$  and  $G_{\text{positive}}$  patients or males and females. The average mitochondrial size was significantly lower in patients with HCM compared with non-failing donors indicative of mitochondrial fragmentation. No sex or genotype differences were observed among patients with HCM (Figure 6C–E). Myofibril area, mitochondrial area, and mitochondrial size were not associated with any mitochondrial function parameter, which is exemplified in Figure 6F–H for OXPHOS capacity. Since mitochondrial fragmentation may be caused by an imbalance between mitochondrial fission and fusion or altered mitophagy,<sup>31</sup> we evaluated abundance of markers of mitochondrial fission (Drp1), fusion (Opa1 and Mfn2), and mitophagy (PINK1 and PARKIN), and additionally consulted a proteomics dataset previously generated using myectomy samples from patients with HCM<sup>16</sup> to assess levels of fission markers (Mff and Fis1) and fusion markers (Opa1 and Mfn2) (see Supplementary material online, Figure S2). Fission did not appear up-regulated in

HCM compared with non-failing hearts, evident from unchanged levels of Mff, Fis1, and Drp1 (see Supplementary material online, Figure S2A and D). Mitochondrial fusion proteins were more abundant in HCM compared with non-failing hearts, apparent from higher levels of Opa1 and Mfn2 (see Supplementary material online, Figure S2B and G). Mitophagy markers PINK1 and PARKIN did not differ between HCM and non-failing donor hearts. Taken together, these findings indicate that mitochondrial fragmentation in HCM is not accompanied by higher expression of fission or mitophagy markers or decreased fusion proteins.

Since disruption of mitochondrial cristae structure is associated with impaired respiration,<sup>32</sup> we also explored whether mitochondrial dysfunction was associated with marked changes in cristae morphology. Supplementary material online, Figure S3A shows representative images from samples with varying degrees of mitochondrial dysfunction and disorganization. No obvious changes in cristae structure (e.g. swelling) were observed in severely affected tissue samples. Additionally, proteomics data of myectomy samples from patients with HCM did not display reduced expression of key regulators of cristae structure (i.e. MICOS proteins, Metaxin1 and -2, Sam50, Dnajc11<sup>33,16</sup>) (see Supplementary material online, Figure S3B). In fact, MICOS subunit 25 was markedly increased in HCM. Thus, these observations do not suggest that remodelling of cristae structure is associated with mitochondrial dysfunction in HCM.



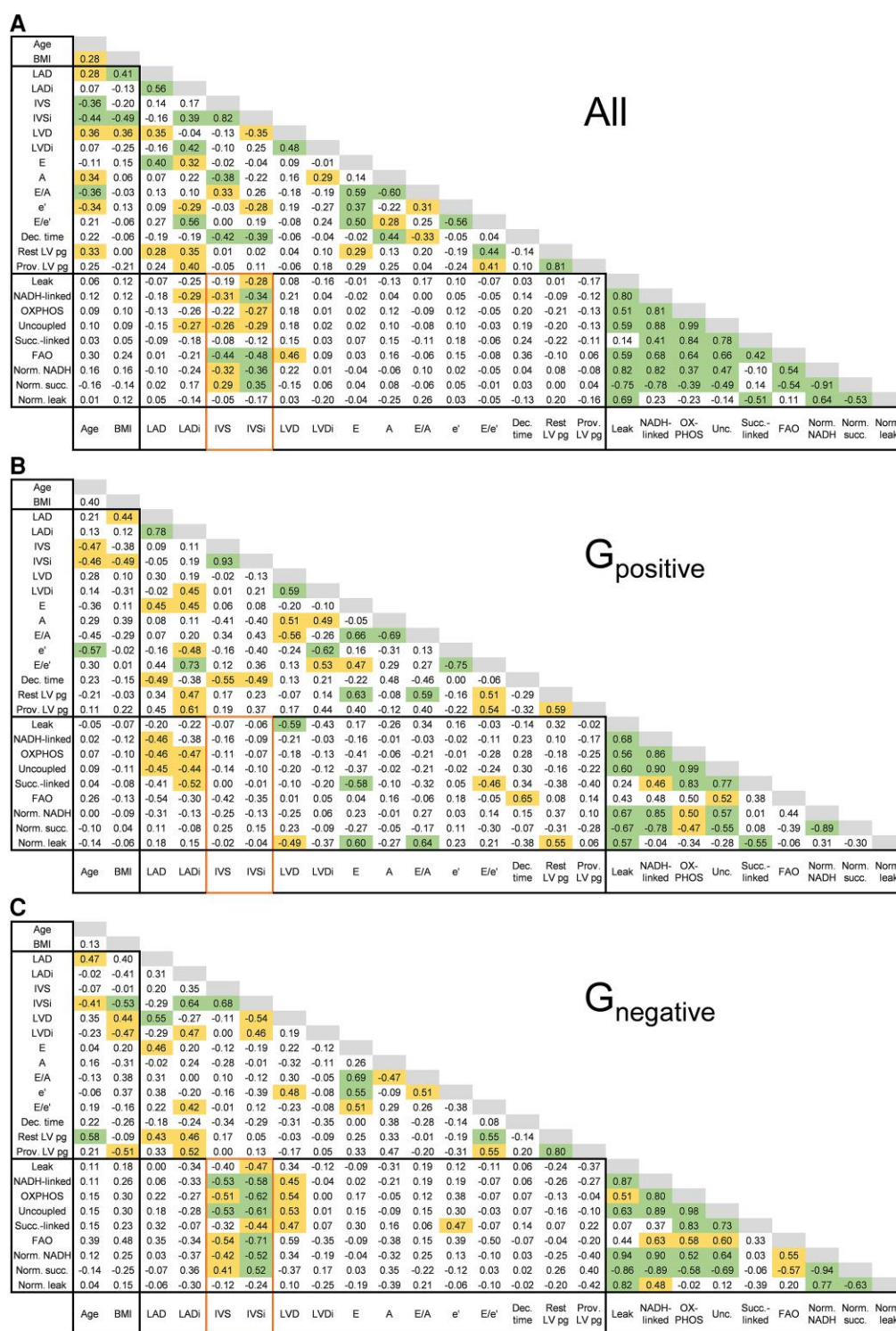


**Figure 4** Correlation matrices showing correlations between clinical, echocardiographic, and mitochondrial function parameters in patients with hypertrophic cardiomyopathy. Matrix A shows correlations of all patients combined; matrix B shows genotype-positive ( $G_{\text{positive}}$ ) patients; matrix C shows genotype-negative ( $G_{\text{negative}}$ ) patients. Values indicate Pearson's  $r$ . Correlations significant at  $P < 0.05$  are marked in yellow; correlations significant at  $P < 0.01$  are marked in green. Correlations between mitochondrial functional parameters and echocardiographic parameters are highlighted by an orange frame. BMI, body mass index; LAD, left atrial diameter; LADi, left atrial diameter indexed to body surface area; IVS, interventricular septum thickness; IVSi, interventricular septum thickness indexed to body surface area; LVD, left ventricular diameter at end-diastole; LVDi, left ventricular diameter at end-diastole indexed to body surface area; Dec. time, deceleration time; Rest LV pg, resting left ventricular outflow tract pressure gradient; Prov. LV pg, left ventricular outflow tract pressure gradient after Valsalva manoeuvre; OXPHOS, total oxidative phosphorylation capacity; Unc., uncoupled respiration; Succ.-linked, succinate-linked respiration; FAO, fatty acid oxidation; Norm. NADH, NADH-linked respiration normalized to OXPHOS; Norm. succ., succinate-linked respiration normalized to uncoupled respiration; Norm. leak, leak respiration normalized to OXPHOS.



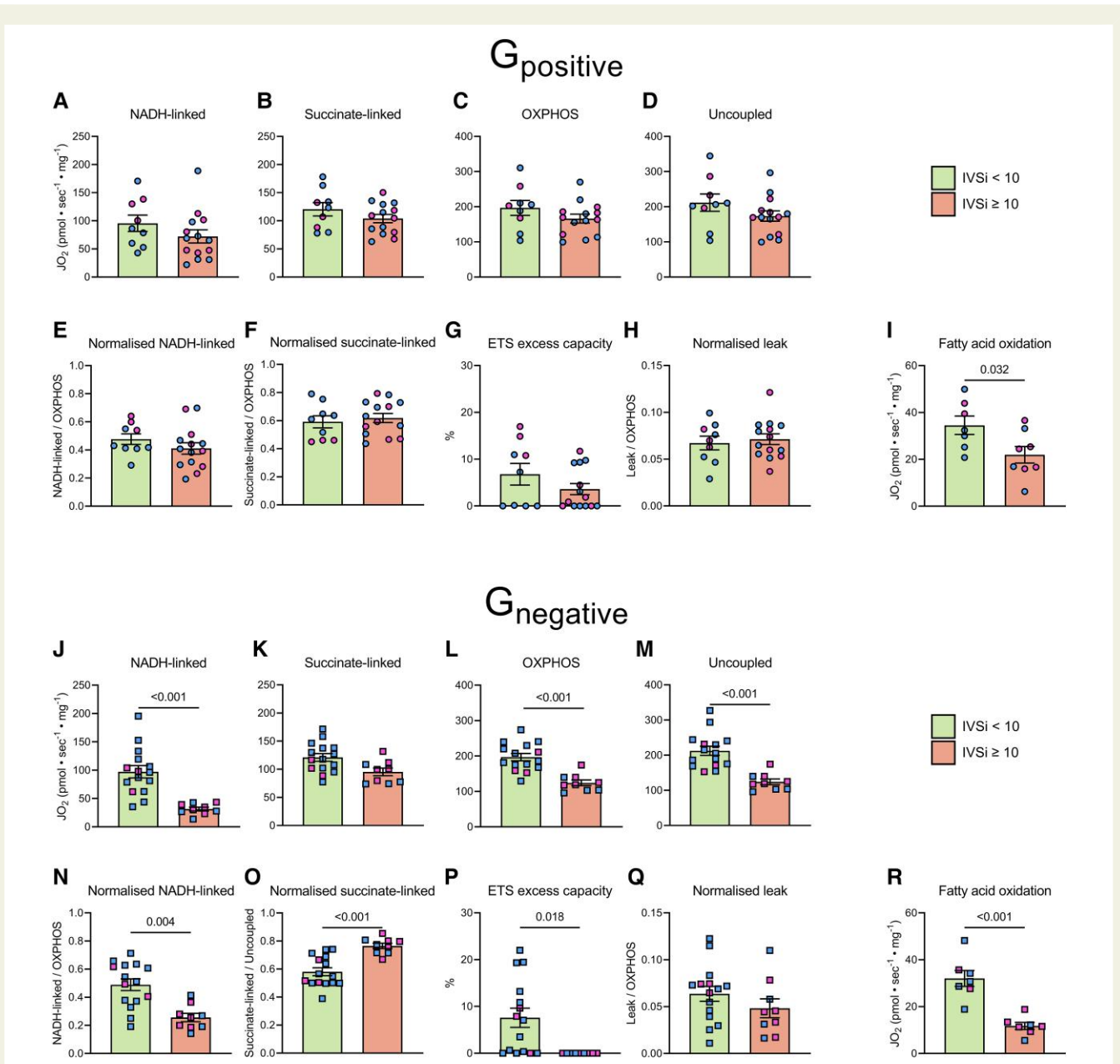


**Figure 5** Mitochondrial respiration in myectomy tissue samples from genotype-negative ( $G_{\text{negative}}$ ) and genotype-positive ( $G_{\text{positive}}$ ) patients with hypertrophic cardiomyopathy with an indexed interventricular septum thickness (IVSi) <10 and ≥10. Parameters in (A–D, I, J–M, and R) represent absolute values. Normalized NADH-linked respiration indicates NADH-linked respiration expressed as a fraction of OXPHOS capacity (E and H). Normalized succinate-linked respiration indicates succinate-linked respiration expressed as a fraction of uncoupled respiration (F and O). Electron transfer system excess capacity indicates the percentage difference between OXPHOS capacity and uncoupled respiration (G and P). Normalized leak indicates leak respiration expressed as a fraction of OXPHOS capacity (H and Q). Data are expressed as mean ± standard error of the mean. Sample sizes:  $G_{\text{positive}}$  patients in (A–H)  $N = 23$  (14 males, 9 females) and (I)  $N = 15$  (8 males, 7 females);  $G_{\text{negative}}$  patients in (J–Q)  $N = 24$  (16 males, 8 females) and (R)  $N = 14$  (7 males, 7 females). Statistical tests: unpaired Student's *t*-test in (B–F, H, I, K–O, Q, and R); Welch's *t*-test in (J); Mann–Whitney test in (A, G, and P). A Bonferroni correction was applied in (A–H and J–Q). Blue and pink symbols indicate male and female patients, respectively.

We also explored whether the expression of OXPHOS protein complex subunits was associated with mitochondrial respiratory function. Compared with non-failing donors patients with HCM displayed lower abundance of complex I subunit NDUF8. Combined levels of OXPHOS protein complex subunits (i.e. the summed intensity of all bands) were lower in patients with HCM vs. non-failing donors, and correlated significantly with OXPHOS

capacity (see [Supplementary material online, Figure S4A–C](#)). Hence, abundance of OXPHOS machinery rather than mitochondrial abundance is a determinant of respiratory capacity. Normalized NADH-linked respiration was not significantly associated with abundance of complex I protein, indicating NADH oxidation capacity is predominantly regulated via mechanisms other than complex I protein levels.

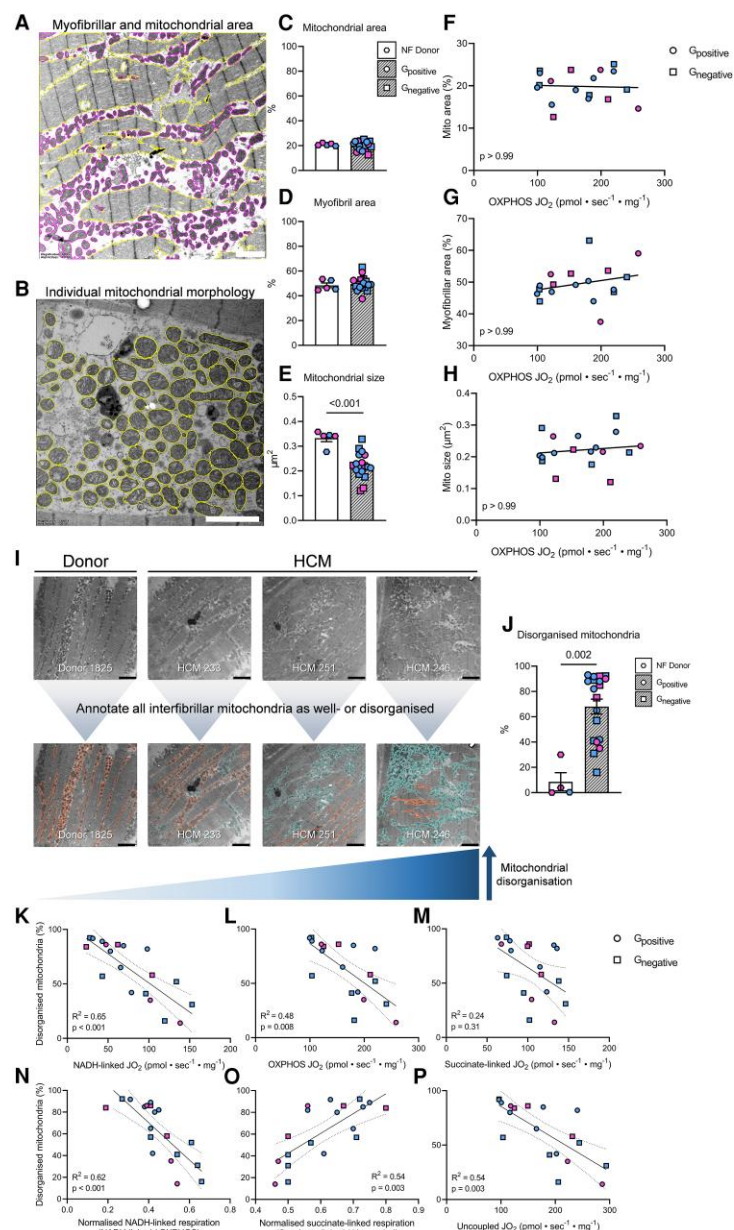


**Figure 6** Overview of transmission electron microscopy analyses in tissue samples from non-failing donor hearts and myectomy samples from patients with hypertrophic cardiomyopathy. (A and B) Examples of how images were annotated to quantify myofibrillar area, mitochondrial area, and individual mitochondrial morphology, the results of which are displayed in (C–E). (F–H) Depict correlations between oxidative phosphorylation (OXPHOS) capacity and myofibrillar area, mitochondrial area, and mitochondrial size in myectomy samples from patients with hypertrophic cardiomyopathy. Examples of TEM images of non-failing donor heart samples and hypertrophic cardiomyopathy myectomy tissue samples in which all interfibrillar mitochondria are annotated; varying degrees of mitochondrial disorganization are visible in hypertrophic cardiomyopathy (I). Percentage disorganized mitochondria in non-failing donor heart tissue and hypertrophic cardiomyopathy myectomy tissue (J). Correlations between percentage disorganized mitochondria and mitochondrial function parameters in myectomy samples from patients with hypertrophic cardiomyopathy (K–P). (K–M and P) Absolute respiration values. Normalized NADH-linked respiration indicates NADH-linked respiration expressed as a fraction of OXPHOS capacity (N). Normalized succinate-linked respiration indicates succinate-linked respiration expressed as a fraction of uncoupled respiration (O). Scale bars indicate 2  $\mu\text{m}$  (A, B, and I). Data are expressed as mean  $\pm$  standard error of the mean. Correlations are displayed as linear regression; dotted lines indicate a 95% confidence interval.  $R^2$  indicates the coefficient of determination. Sample sizes: non-failing donors  $N = 5$  (2 males, 3 females); genotype-positive ( $G_{\text{positive}}$ ) patients  $N = 10$  (7 males, 3 females); genotype-negative ( $G_{\text{negative}}$ ) patients  $N = 8$  (5 males, 3 females) in (C–H). Non-failing donors  $N = 5$  (2 males, 3 females);  $G_{\text{positive}}$  patients  $N = 10$  (7 males, 3 females);  $G_{\text{negative}}$  patients  $N = 9$  (6 males, 3 females) in J.  $G_{\text{positive}}$  patients  $N = 10$  (7 males, 3 females);  $G_{\text{negative}}$  patients  $N = 9$  (6 males, 3 females) in (K–P). Statistical tests: Welch's  $t$ -test in (C); unpaired Student's  $t$ -test in (D, E, and J). Bonferroni corrections were applied to all group comparisons (C–E and J) and to all correlations (F–H and K–P). Blue and pink symbols indicate male and female patients, respectively.

## Mitochondrial dysfunction is related to disorganization of interfibrillar mitochondria

Myectomy samples from patients with HCM did not differ from non-failing donors in terms of abundance of myofibrils and mitochondria; however, a striking difference appeared to be the structural organization of IF mitochondria relative to the myofilaments. In non-failing donor samples, IF mitochondria were consistently properly organized in strands parallel to myofibrils. In HCM samples such organization was frequently disrupted, typified by distribution patterns of IF mitochondria disconnected from myofibrillar organization, and by the formation of isolated clusters of IF mitochondria (Figure 6I, see [Supplementary material online, Figure S6](#)). In non-failing donor samples, clustering was also observed, but these typically appeared where separate strands of properly organized IF mitochondria converge (see [Supplementary material online, Figure S6](#)). We quantified the severity of so-called mitochondrial disorganization by calculating the average percentage of disorganized mitochondria in a subset of samples. In HCM, the percentage of disorganized mitochondria was eight-fold higher than in non-failing donors. The percentage of disorganized mitochondria correlated significantly with NADH-linked respiration, OXPHOS capacity, uncoupled respiration, normalized NADH-linked respiration, and normalized succinate-linked respiration (Figure 6J–P). Hence, these data suggest proper organization of IF mitochondria relative to myofibrils is required to safeguard mitochondrial respiratory capacity. Cardiac mitochondria are transported along microtubules,<sup>34</sup> which are markedly more abundant in the HCM myocardium.<sup>16</sup> Microtubules moreover undergo extensive modification by means of acetylation and deetyrosination, increasing microtubule flexibility and stability, respectively.<sup>35,36</sup> We explored whether mitochondrial disorganization was associated with tubulin alterations. In line with previous reports,<sup>16,37</sup> we found higher levels of total, acetylated, and deetyrosinated  $\alpha$ -tubulin in HCM vs. non-failing tissue, but none of these parameters displayed associations with mitochondrial disorganization (see [Supplementary material online, Figure S7 and Table S2](#)).

## Elamipretide and increasing NAD<sup>+</sup> levels both improve mitochondrial function ex vivo

We applied two strategies to improve mitochondrial respiration *ex vivo*, thereby aiming to identify possible therapeutic treatment targets.

In myectomy samples from patients with HCM, defects in NAD<sup>+</sup> homeostasis have been identified,<sup>16</sup> suggesting mitochondrial NAD<sup>+</sup> levels may be reduced, lowering the availability of NAD<sup>+</sup> for conversion to NADH and contributing to bioenergetic impairment. To assess whether NADH-linked respiration in HCM is limited by mitochondrial NAD<sup>+</sup> levels, we tested in a subset of samples ( $n = 13$ ) whether directly increasing NAD<sup>+</sup> levels boosted respiration (Figure 7). All samples displayed a robust increase in NADH-linked respiration upon the addition of NAD<sup>+</sup>. Moreover, the increase in respiration was proportional to the severity of impairment as evaluated prior to the addition of NAD<sup>+</sup> (Figure 7C and D). Since raising mitochondrial NAD<sup>+</sup> may activate mitochondrial NAD<sup>+</sup>-dependent deacetylases,<sup>38</sup> we evaluated mitochondrial protein acetylation in fresh saponin-permeabilized myectomy samples ( $n = 3$ ) in response to NAD<sup>+</sup> treatment. However, no change in

mitochondrial protein acetylation was observed (see [Supplementary material online, Figure S9](#)).

In HCM, it has been hypothesized that mitochondrial respiratory function is compromised due to cardiolipin peroxidation and concomitant disruption of respiratory supercomplex formation.<sup>17,39</sup> Treatment with the cardiolipin-stabilizing compound elamipretide may ameliorate energetic impairment and oxidative stress in HCM via improving respiratory supercomplex assembly.<sup>21</sup> Analogous to the approach of Chatfield et al.,<sup>24</sup> who demonstrated a beneficial effect of elamipretide on respiratory function in explanted failing myocardium, we incubated myectomy tissue samples and measured flux through OXPHOS pathways in the presence of 100  $\mu$ M elamipretide (Figure 8). NADH-linked respiration was significantly increased in response to elamipretide treatment, whereas succinate-linked respiration was unchanged. Accordingly, normalized NADH-linked respiration was higher and normalized succinate-linked respiration was decreased upon elamipretide treatment (Figure 8C–J). The restorative effect of elamipretide was particularly apparent in samples that displayed impaired NADH-linked respiration at baseline (Figure 8K). Analysis of respiratory supercomplex composition via Blue Native gel electrophoresis revealed that elamipretide-treated tissue displayed higher amounts of respiratory supercomplexes containing complex I (Figure 8L and M). Taken together, these findings suggest that elamipretide may have a significant beneficial effect on respiratory capacity, which is mediated through enhanced incorporation of complex I into respiratory supercomplexes, thereby improving the capacity to oxidize NADH.

## Discussion

Here, we performed mitochondrial respiration measurements in a large number of cardiac tissue samples from patients with HCM to characterize mitochondrial function at the time of myectomy and identify patient group-specific mitochondrial changes. Mitochondrial performance varied greatly among patients, which was not explained by genotype, sex, age, or BMI. In  $G_{\text{negative}}$  patients, but not  $G_{\text{positive}}$  patients, mitochondrial function was negatively associated with septal thickness. At the cellular level, disorganization of mitochondria was found to be related to mitochondrial dysfunction. Despite this disrupted organization, mitochondrial function could be boosted via treatment strategies using NAD<sup>+</sup> and elamipretide, eliciting the mitochondria as the potential druggable target to ameliorate or prevent cardiac remodelling in HCM ([Structured Graphical Abstract](#)). Taken together, this report is the first to comprehensively characterize mitochondrial function alterations in HCM and how these are linked to clinical phenotype and cardiomyocyte ultrastructure, and demonstrates therapeutic potential of the mitochondria in a human setting.

## Associations between mitochondrial function and clinical characteristics

Our investigation shows that on average no differences in mitochondrial function exist between  $G_{\text{positive}}$  and  $G_{\text{negative}}$  patients with HCM at the time of myectomy. Functional impairment might be expected to be more pronounced in  $G_{\text{positive}}$  than in  $G_{\text{negative}}$  HCM, given the sarcomere mutation-induced myofilament defects in  $G_{\text{positive}}$  patients that lead to increased ATP consumption and mitochondrial stress.<sup>7–12</sup> This suggests that at the time of myectomy mitochondrial dysfunction is a common feature among all patients with HCM, the severity of which is not impacted by the primary aetiology of the disease. This is in line with previous reports showing that metabolic derailment

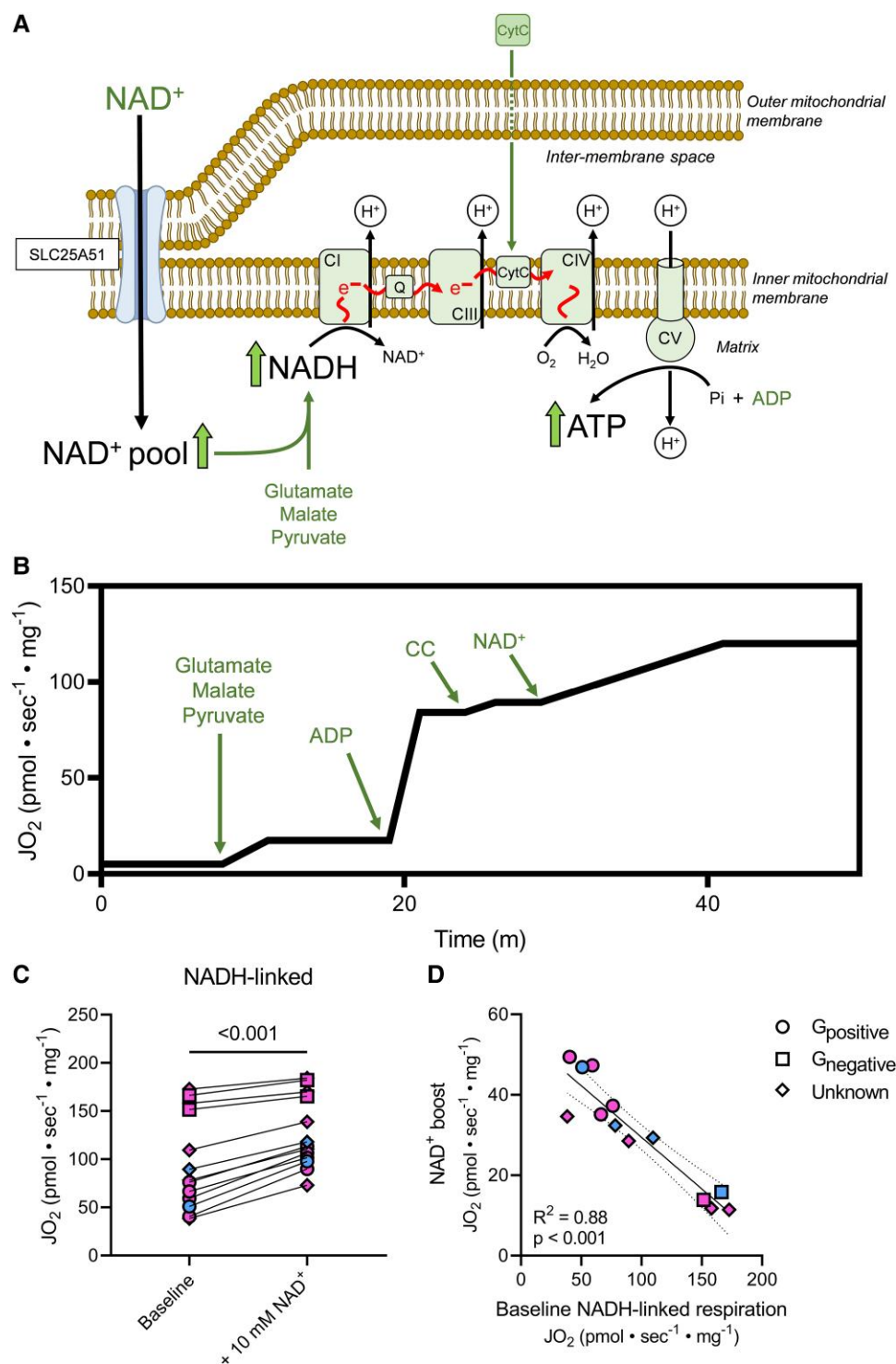


**Figure 7** Effect of NAD<sup>+</sup> supplementation on mitochondrial function ex vivo in myectomy samples from patients with hypertrophic cardiomyopathy. (A) The proposed mechanism via which NAD<sup>+</sup> supplementation boosts the capacity of NADH-linked respiration. NAD<sup>+</sup> enters the mitochondrial matrix via SLC25A51, raising the mitochondrial NAD<sup>+</sup> pool and increasing NAD<sup>+</sup> availability for NADH production and subsequent respiration via complex I. Average trace during the experimental protocol is shown in (B). The absolute rate of NADH-linked respiration before and after adding NAD<sup>+</sup> is seen in (C) (paired two-tailed t-test). (D) The association between NADH-linked respiration before adding NAD<sup>+</sup> and the absolute respiration increase that followed upon adding NAD<sup>+</sup>. Correlation is displayed as linear regression; dotted lines indicate a 95% confidence interval.  $R^2$  indicates the coefficient of determination. Sample sizes:  $N = 13$  (4 males, 9 females) in (C and D). Blue and pink symbols indicate male and female patients, respectively. G<sub>positive</sub>, genotype-positive; G<sub>negative</sub>, genotype-negative.



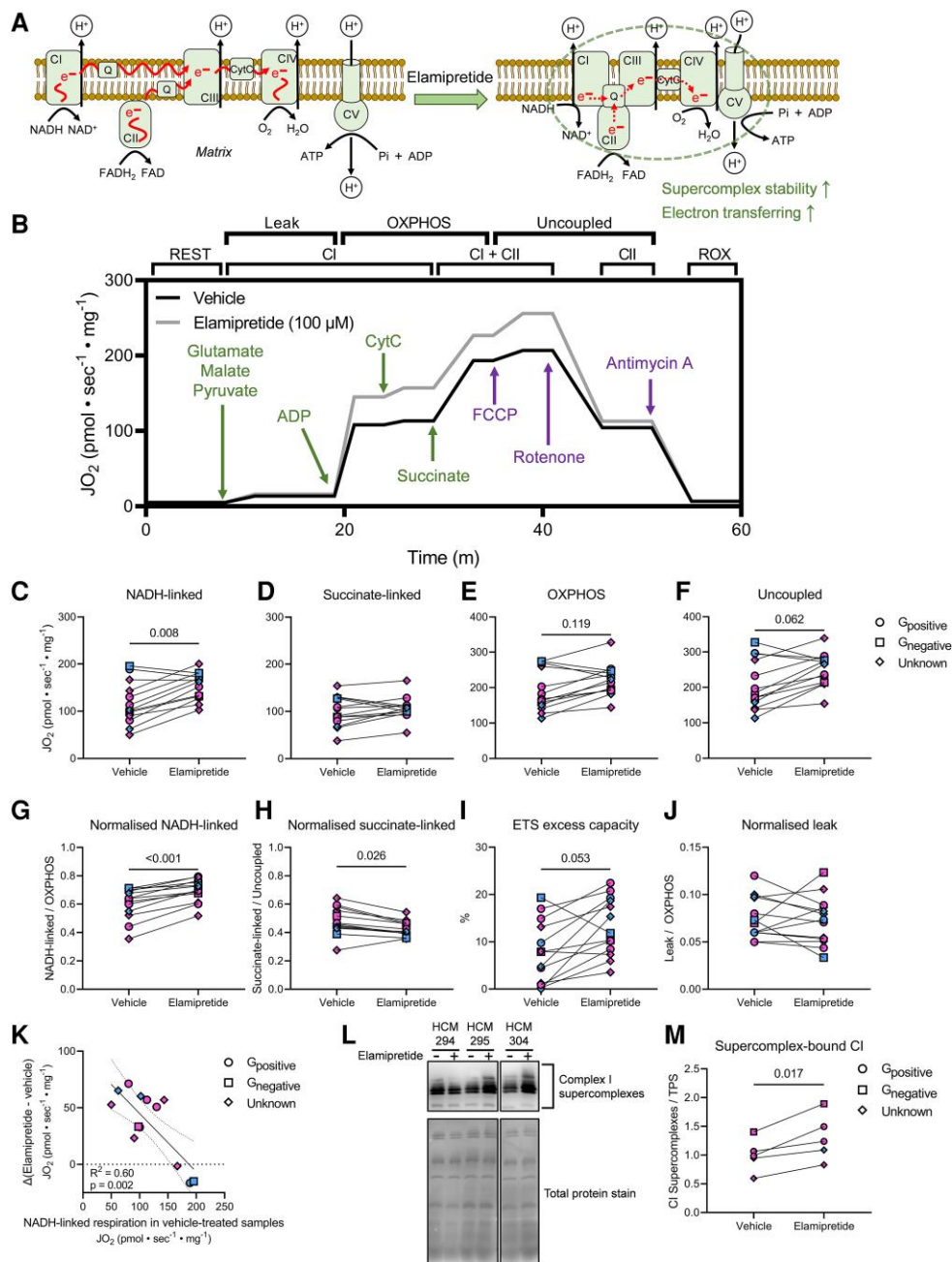


**Figure 8** Effect of elamipretide incubation on mitochondrial function ex vivo in myectomy samples from patients with hypertrophic cardiomyopathy. (A) The proposed mechanism via which elamipretide improves mitochondrial respiratory function. Elamipretide associates with cardiolipin, stabilizing respiratory supercomplexes which ameliorates electron transfer through complexes. Average traces for both treatment conditions during the experimental protocol are shown in (B). (C–F) Absolute respiration values. Normalized NADH-linked respiration indicates NADH-linked respiration expressed as a fraction of OXPHOS capacity (G). Normalized succinate-linked respiration indicates succinate-linked respiration expressed as a fraction of uncoupled respiration (H). Electron transfer system (ETS) excess capacity indicates the percentage difference between OXPHOS capacity and uncoupled respiration (I). Normalized leak indicates leak respiration expressed as a fraction of OXPHOS capacity (J). (K) The association between NADH-linked respiration in vehicle-treated samples and the absolute difference in NADH-linked respiration relative to the matched elamipretide-treated samples. Representative Blue Native gel electrophoresis lanes showing supercomplex-bound complex I in myectomy samples from patients with hypertrophic cardiomyopathy that were treated with vehicle or 100  $\mu\text{M}$  elamipretide (L); quantification in (M). Treatment effects were analysed using the paired two-tailed *t*-test (C–J and M). A Bonferroni correction was applied in (C–J). Correlation (K) is displayed as linear regression; dotted lines indicate a 95% confidence interval.  $R^2$  indicates the coefficient of determination. Sample sizes:  $N = 13$  (4 males, 9 females) in (C–K);  $N = 5$  (1 male, 4 females) in (L and M). Blue and pink symbols indicate male and female patients, respectively. CytC, cytochrome-c; FCCP, carbonyl cyanide *p*-trifluoromethoxyphenyl hydrazine; ROX, residual oxygen consumption;  $G_{\text{positive}}$ , genotype-positive;  $G_{\text{negative}}$ , genotype-negative; TPS, total protein stain.

is a key hallmark of the disease, occurring independently of sarcomere mutation status.<sup>16,17,40</sup> Similarly, age and body weight, which are associated with increased penetrance and aggravation of disease,<sup>41–44</sup> did not correlate with severity of mitochondrial dysfunction at a time point of disease when patients present with symptomatic LVOT obstruction. We also found no sex differences in mitochondrial function, despite the fact that female patients with HCM display worse diastolic impairment and cardiac remodelling than male patients at the time of myectomy.<sup>28</sup> Several (mitochondrial) sex differences that are thought to confer cardioprotective effects in females have been described,<sup>45</sup> which may explain why female patients do not display worse mitochondrial dysfunction than men.

In  $G_{\text{negative}}$  patients, OXPHOS-linked parameters and fatty acid oxidation capacity displayed a strong negative association with septal hypertrophy. Thus, in  $G_{\text{negative}}$  HCM impairment of mitochondrial respiration and substrate inflexibility appear to be tightly linked to cardiac remodelling. Due to the availability of tissue samples only at one clinical endpoint in this study, we cannot establish whether mitochondrial dysfunction plays a causative role in hypertrophic remodelling. However, mitochondrial cardiomyopathies, in which primary mitochondrial defects cause disease, typically precipitate an HCM-like phenotype;<sup>46</sup> therefore, we speculate that mitochondrial dysfunction may be a driver of disease in  $G_{\text{negative}}$  HCM. Models that recapitulate  $G_{\text{negative}}$  HCM are lacking, thus disease-driving potential of mitochondrial impairment should be studied by linking the mitochondrial phenotype at the time of myectomy to long-term follow-up. In  $G_{\text{positive}}$  patients, only fatty acid oxidation capacity was lower in patients with an IVSi  $\geq 10$  vs. IVSi  $< 10$ . Thus, in  $G_{\text{positive}}$  HCM, septal hypertrophy does not appear to be a reflection of impaired mitochondrial performance and may rather represent a maladaptive response to inefficient myofilament function caused by mutant sarcomere proteins. The finding of lower fatty acid oxidation capacity in  $G_{\text{positive}}$  patients with an IVSi  $\geq 10$  vs. IVSi  $< 10$  is consistent with a shift from fatty acids towards glucose as the preferred energy source that typically occurs in cardiac hypertrophy.<sup>47</sup>

## Diminished NADH-linked respiration is the main functional defect of hypertrophic cardiomyopathy

Our analyses show that as overall mitochondrial respiratory capacity (i.e. OXPHOS) deteriorates NADH-linked respiration makes up a smaller proportion of OXPHOS capacity, suggesting an impaired capacity to oxidize NADH is the most prominent mitochondrial defect. A recent investigation also showed oxygen flux in isolated mitochondria was depressed in response to NADH-producing substrates glutamate and malate and ADP in a small number of HCM myectomy samples ( $n=5$ ) compared with non-failing donor samples, but did not evaluate flux under different substrate combinations.<sup>17</sup> A study in feline HCM revealed that NADH-linked respiration in permeabilized cardiac tissue was  $\geq 50\%$  lower in HCM hearts compared with non-failing hearts.<sup>19</sup> Proteomic analyses in HCM myectomy samples furthermore demonstrated reduced abundance of OXPHOS proteins, which was most striking for subunits of complex I.<sup>16</sup> The finding that NADH-linked rather than succinate-linked respiratory capacity is dysfunctional in human HCM implies severe consequences for bioenergetics, since succinate-driven respiration has been found to possess a large *ex vivo* reserve capacity of up to 90% that is not utilized *in vivo*.<sup>48</sup>

## Ultrastructural correlates of mitochondrial dysfunction

Our TEM analyses revealed smaller mitochondrial size compared with controls without a change in mitochondrial area suggestive of mitochondrial fragmentation, the severity of which was not related to mitochondrial function. In line with previous work,<sup>17</sup> our findings yielded no indications for up-regulation of mitochondrial fission or mitophagy, but rather imply up-regulation of fusion-related proteins, which may reflect an attempt to counteract excessive mitochondrial fragmentation. Thus, the mechanisms that mediate mitochondrial fragmentation in HCM remain unclear and may occur early in HCM pathogenesis, warranting further study in mouse and human stem cell-derived models of HCM. Mitochondrial abundance was unchanged in HCM compared with non-failing donors, which was also observed by others.<sup>17</sup> Diminished respiratory capacity was not associated with loss of mitochondria, underscoring the importance of mitochondrial quality rather than number in facilitating proper respiratory capacity.

Strikingly, we found mitochondrial function to be strongly related to the disorganization of IF mitochondria, presenting as aberrant clustering and/or loss of proper alignment to myofilaments. To the best of our knowledge, our study is the first to report a negative association between mitochondrial respiratory function and spatial organization of IF mitochondria in human cardiac tissue. A previous study in patients with HCM demonstrated that impaired contractile and relaxation reserve was associated with an increase in average distance from mitochondria to the nearest myofilament, which may indicate a link between mitochondrial dysfunction and abnormal clustering (i.e. disorganization).<sup>49</sup> Mitochondrial clustering is also observed in patients with mitral regurgitation and preserved ventricular function,<sup>50</sup> and in animal models of right ventricular heart failure, pressure/volume overload-induced heart failure, tachypacing-induced heart failure, and diabetic cardiomyopathy,<sup>51–57</sup> suggesting mitochondrial disorganization in heart disease is a general pathological response. Proper organization of mitochondria is required for efficient phosphocreatine provision to the myofilaments to support contraction and relaxation.<sup>58</sup> In addition, mitochondria require close proximity to the sarcoplasmic and endoplasmic reticulum to maintain calcium homeostasis,<sup>59,60</sup> which is important in responding adequately to changes in cardiac workload.<sup>61</sup> Analyses in an ovine model of tachypacing-induced heart failure showed that disorganization of IF mitochondria coincided with disruption of the structural relationship between the sarcoplasmic reticulum and mitochondria.<sup>56</sup> Thus, mitochondrial disorganization in HCM may be linked to impaired mitochondria–sarcoplasmic reticulum cross-talk, compromising mitochondrial bioenergetics, reactive oxygen species (ROS) defence, and calcium-cycling. Cardiac mitochondria have also been demonstrated to form communicative networks that facilitate propagation and synchronization of ROS-signalling and mitochondrial membrane potential,<sup>62</sup> which may be important in ensuring physiological ROS-mediated cardioprotective processes such as mitochondrial quality control.<sup>63,64</sup> In a guinea-pig model of heart failure displaying mitochondrial disorganization such network behaviour was disrupted.<sup>54</sup> Impaired mitochondrial network communication may thus represent an additional pathophysiological mechanism in HCM disease progression. In cardiomyocytes, the microtubule cytoskeleton facilitates mitochondrial movement;<sup>34</sup> however, we observed no relations between mitochondrial disorganization and amounts of (post-translationally modified) tubulin. Thus, the mechanisms associated with mitochondrial disorganization remain unclear and warrant further study. Taken together, our observation of disrupted mitochondrial organization in cardiac tissue from patients with obstructive HCM indicates that this

represents a relatively early pathological change in HCM disease progression, which may have multiple adverse consequences for cardiomyocyte function and homeostasis. An improved understanding of the mechanisms driving mitochondrial disorganization may aid in designing therapeutic strategies aimed at preserving cardiomyocyte architecture.

## Improving mitochondrial function as a potential treatment strategy in hypertrophic cardiomyopathy

In this study, we deployed two approaches to demonstrate the therapeutic potential of the mitochondria in HCM myocardium. Supplementation with NAD<sup>+</sup> significantly improved NADH-linked respiration in HCM myectomy tissue. The increase in respiration upon stimulation with NAD<sup>+</sup> was most pronounced in patient samples that displayed the worst degree of impairment at baseline. In HEK293T cells, NAD<sup>+</sup> boosted respiration only when mitochondrial NAD<sup>+</sup> levels were depleted.<sup>65</sup> Combined, these findings suggest that the NAD<sup>+</sup>-induced respiration boost in HCM myectomy samples is a reflection of the depressed capacity to produce and consume NADH, and do not imply the existence of a supraphysiological reserve of NADH-linked respiration capacity. Acetylation of mitochondrial proteins was unchanged in response to NAD<sup>+</sup>-treatment, suggesting the acute boosting effect of NAD<sup>+</sup> on NADH-linked respiration cannot be explained by an immediate increase in sirtuin-mediated deacetylation.<sup>38</sup> Rather, the effect of NAD<sup>+</sup> supplementation on NADH-linked respiration implies that lowered mitochondrial NAD<sup>+</sup> levels may be a major rate-limiting factor to produce NADH. NADH production may also be lowered as a consequence of reduced abundance of Krebs cycle dehydrogenases and insufficient mitochondrial calcium uptake in HCM,<sup>12,16</sup> which may in part be compensated by increasing mitochondrial NAD<sup>+</sup> levels. Further study is warranted to unveil whether strategies using NAD<sup>+</sup> precursors, e.g. the recently introduced potent NAD<sup>+</sup> precursor NMNH (reduced nicotinamide mononucleotide),<sup>66</sup> may improve or prevent disease phenotypes in experimental models of HCM through increasing mitochondrial NAD<sup>+</sup> levels and beneficial cardiometabolic effects mediated by activation of NAD<sup>+</sup>-dependent sirtuin enzymes.<sup>67</sup>

Elamipretide is a small tetrapeptide that selectively targets the mitochondrial membrane-specific phospholipid cardiolipin.<sup>21</sup> Cardiolipin stabilizes respiratory supercomplexes and inhibits peroxidase activity of cytochrome-c, thereby facilitating optimal ATP synthesis while limiting ROS production.<sup>68</sup> Also, cardiolipin may be a key regulator of the active-to-deactive transition of complex I, i.e. complex I activation depends on binding to cardiolipin.<sup>69</sup> Elamipretide has been shown to improve cardiac function in rodent and canine models of heart failure.<sup>70,71</sup> More recently, elamipretide was reported to ameliorate mitochondrial function in explanted failing myocardium, which coincided with improved supercomplex function.<sup>24</sup> In HCM, it is hypothesized that peroxidation of cardiolipin destabilizes supercomplexes, contributing to energetic impairment and oxidative stress.<sup>17,39</sup> Compounds that enhance the effects of cardiolipin may, therefore, potentially support bioenergetics and restore redox state alterations in HCM. Here, we show that treating fresh HCM myectomy tissue with elamipretide increased complex I incorporation into respiratory supercomplexes and ameliorated overall mitochondrial performance via improved NADH-linked respiration. This suggests that functional impairment of NADH-linked respiration in HCM is partly explained by inefficient coupling of complex I to complexes III and IV, which may be linked to depressed respiratory supercomplex formation and complex I inactivation.

## Study limitations and clinical implications

Mitochondrial respiratory function was not studied in non-failing hearts as fresh tissue was unavailable, thus we could not determine how functional alterations in HCM compare to healthy hearts. Instead, we linked mitochondrial performance to clinical aspects of disease to gain insight into the role of mitochondrial impairment in HCM pathophysiology. In G<sub>negative</sub> patients, mitochondrial dysfunction was strongly linked to septal growth, whereas in G<sub>positive</sub> patients, hypertrophy may rather occur in response to sarcomere mutation-induced myofilament inefficiency. Due to the availability of tissue only at the time of myectomy, we cannot establish a causal relationship between mitochondrial dysfunction and hypertrophy. Nevertheless, we propose that particularly in G<sub>negative</sub> patients targeting mitochondrial function may halt and reverse disease progression, whereas in G<sub>positive</sub> patients, correcting sarcomere mutation-mediated myofilament dysfunction may be more effective. Indeed, in the EXPLORER-HCM trial, which evaluated the effectiveness of the myosin-inhibitor mavacamten, a larger percentage of G<sub>positive</sub> patients with HCM met the primary endpoint than G<sub>negative</sub> patients.<sup>72</sup>

## Conclusions

Mitochondrial impairment in HCM is associated with disrupted cardiomyocyte architecture and is linked to septal hypertrophy in G<sub>negative</sub> patients. Impaired NADH-linked respiration represented the main mitochondrial respiratory defect and could be boosted by raising mitochondrial NAD<sup>+</sup> levels and by elamipretide treatment. Mitochondria-targeted therapy may prevent or ameliorate cardiac disease, particularly in G<sub>negative</sub> patients with HCM, given the tight link between mitochondrial impairment and septal thickening in this subpopulation. Our data provide proof for the potential of mitochondrial drugs in the treatment of HCM and further studies are warranted.

## Acknowledgements

We thank Willemijn op den Brouw and Roy Huurman for technical assistance and Prof. Mark van de Wiel for statistical input. Figures were created with BioRender.com.

## Supplementary data

Supplementary data is available at *European Heart Journal* online.

## Pre-registered clinical trial number

None supplied.

## Ethical approval statement

Ethical approval was not required.

## Data availability statement

The data underlying this article will be shared on reasonable request to the corresponding author.

## Conflict of interest statement

K.B.M. is a consultant for Bristol Myers Squibb and receives research support from Amgen.

## Funding statement

We acknowledge support from the Netherlands Organization for Scientific Research (NWO VICI, grant 91818602) and the Leducq Foundation (20CVD01).

## References

- Semsarian C, Ingles J, Maron MS, Maron BJ. New perspectives on the prevalence of hypertrophic cardiomyopathy. *J Am Coll Cardiol* 2015;**65**:1249–1254. <https://doi.org/10.1016/j.jacc.2015.01.019>
- Ommen SR, Mital S, Burke MA, Day SM, Deswal A, Elliott P, et al. 2020 AHA/ACC guideline for the diagnosis and treatment of patients with hypertrophic cardiomyopathy: a report of the American College of Cardiology/American Heart Association Joint Committee on Clinical Practice Guidelines. *J Am Coll Cardiol* 2020;**76**:e159–e240. <https://doi.org/10.1016/j.jacc.2020.08.045>
- Maron BJ. Clinical course and management of hypertrophic cardiomyopathy. *N Engl J Med* 2018;**379**:1977. <https://doi.org/10.1056/NEJMra1710575>
- Ho CY, Charron P, Richard P, Girolami F, Van Spaendonck-Zwarts KY, Pinto Y. Genetic advances in sarcomeric cardiomyopathies: state of the art. *Cardiovasc Res* 2015;**105**:397–408. <https://doi.org/10.1093/cvr/cvv025>
- Neubauer S, Kolm P, Ho CY, Kwong RY, Desai MY, Dolman SF, et al. Distinct subgroups in hypertrophic cardiomyopathy in the NHLBI HCM registry. *J Am Coll Cardiol* 2019;**74**:2333–2345. <https://doi.org/10.1016/j.jacc.2019.08.1057>
- Watkins H. Time to think differently about sarcomere-negative hypertrophic cardiomyopathy. *Circulation* 2021;**143**:2415–2417. <https://doi.org/10.1161/CIRCULATIONAHA.121.053527>
- Sequeira V, Wijnter PJM, Nijenkamp LLAM, Kuster DWD, Najafi A, Witjas-Paalberends ER, et al. Perturbed length-dependent activation in human hypertrophic cardiomyopathy with missense sarcomeric gene mutations. *Circ Res* 2013;**112**:1491–1505. <https://doi.org/10.1161/CIRCRESAHA.111.300436>
- Witjas-Paalberends ER, Ferrara C, Scellini B, Piroddi N, Montag J, Tesi C, et al. Faster cross-bridge detachment and increased tension cost in human hypertrophic cardiomyopathy with the R403Q MYH7 mutation. *J Physiol* 2014;**592**:3257–3272. <https://doi.org/10.1113/jphysiol.2014.274571>
- Witjas-Paalberends ER, Guclu A, Germans T, Knaapen P, Harms HJ, Vermeer AMC, et al. Gene-specific increase in the energetic cost of contraction in hypertrophic cardiomyopathy caused by thick filament mutations. *Cardiovasc Res* 2014;**103**:248–257. <https://doi.org/10.1093/cvr/cvu127>
- Sequeira V, Najafi A, McConnell M, Fowler ED, Bollen IAE, Wust RCL, et al. Synergistic role of ADP and Ca(2+) in diastolic myocardial stiffness. *J Physiol* 2015;**593**:3899–3916. <https://doi.org/10.1113/jp270354>
- Toepfer CN, Garfinkel AC, Venturini G, Wakimoto H, Repetti G, Alamo L, et al. Myosin sequestration regulates sarcomere function, cardiomyocyte energetics, and metabolism, informing the pathogenesis of hypertrophic cardiomyopathy. *Circulation* 2020;**141**:828–842. <https://doi.org/10.1161/CIRCULATIONAHA.119.042339>
- Sequeira V, Bertero E, Maack C. Energetic drain driving hypertrophic cardiomyopathy. *FEBS Lett* 2019;**593**:1616–1626. <https://doi.org/10.1002/1873-3468.13496>
- Crilly JG, Boehm EA, Blair E, Rajagopalan B, Blamire AM, Styles P, et al. Hypertrophic cardiomyopathy due to sarcomeric gene mutations is characterized by impaired energy metabolism irrespective of the degree of hypertrophy. *J Am Coll Cardiol* 2003;**41**:1776–1782. [https://doi.org/10.1016/S0735-1097\(02\)03009-7](https://doi.org/10.1016/S0735-1097(02)03009-7)
- Guclu A, Knaapen P, Harms HJ, Parbhudayal RY, Michels M, Lammertsma AA, et al. Disease stage-dependent changes in cardiac contractile performance and oxygen utilization underlie reduced myocardial efficiency in human inherited hypertrophic cardiomyopathy. *Circ Cardiovasc Imaging* 2017;**10**:e005604. <https://doi.org/10.1161/CIRCIMAGING.116.005604>
- Parbhudayal RY, Harms HJ, Michels M, van Rossum AC, Germans T, van der Velden J. Increased myocardial oxygen consumption precedes contractile dysfunction in hypertrophic cardiomyopathy caused by pathogenic TNNT2 gene variants. *J Am Heart Assoc* 2020;**9**:e015316. <https://doi.org/10.1161/JAHA.119.015316>
- Schuldt M, Peijl, Harakalova M, Dorsch LM, Schlossarek S, Mokry M, et al. Proteomic and functional studies reveal deetyrosinated tubulin as treatment target in sarcomere mutation-induced hypertrophic cardiomyopathy. *Circ Heart Fail* 2021;**14**:e007022. <https://doi.org/10.1161/CIRCHEARTFAILURE.120.007022>
- Ranjbarvaziri S, Kooiker KB, Ellenberger M, Fajardo G, Zhao M, Vander Roest AS, et al. Altered cardiac energetics and mitochondrial dysfunction in hypertrophic cardiomyopathy. *Circulation* 2021;**144**:1714–1731. <https://doi.org/10.1161/CIRCULATIONAHA.121.053575>
- Lucas DT, Aryal P, Szweda LI, Koch WJ, Leinwand LA. Alterations in mitochondrial function in a mouse model of hypertrophic cardiomyopathy. *Am J Physiol Heart Circ Physiol* 2003;**284**:H575–H583. <https://doi.org/10.1152/ajpheart.00619.2002>
- Christiansen LB, Dela F, Koch J, Hansen CN, Leifsson PS, Yokota T. Impaired cardiac mitochondrial oxidative phosphorylation and enhanced mitochondrial oxidative stress in feline hypertrophic cardiomyopathy. *Am J Physiol Heart Circ Physiol* 2015;**308**:H1237–H1247. <https://doi.org/10.1152/ajpheart.00727.2014>
- Michels M, Olivetto I, Asselbergs FW, van der Velden J. Life-long tailoring of management for patients with hypertrophic cardiomyopathy: awareness and decision-making in changing scenarios. *Neth Heart J* 2017;**25**:186–199. <https://doi.org/10.1007/s12471-016-0943-2>
- Szeto HH. First-in-class cardiolipin-protective compound as a therapeutic agent to restore mitochondrial bioenergetics. *Br J Pharmacol* 2014;**171**:2029–2050. <https://doi.org/10.1111/bph.12461>
- van Velzen HG, Schinkel AFL, Baart SJ, Huurman R, van Slegtenhorst MA, Kardys I, et al. Effect of gender and genetic mutations on outcomes in patients with hypertrophic cardiomyopathy. *Am J Cardiol* 2018;**122**:1947–1954. <https://doi.org/10.1016/j.amjcard.2018.08.040>
- Chen CY, Caporizzo MA, Bedi K, Vite A, Bogush AI, Robison P, et al. Suppression of deetyrosinated microtubules improves cardiomyocyte function in human heart failure. *Nat Med* 2018;**24**:1225–1233. <https://doi.org/10.1038/s41591-018-0046-2>
- Chatfield KC, Sparagna GC, Chau S, Phillips EK, Ambardekar AV, Aftab M, et al. Elamipretide improves mitochondrial function in the failing human heart. *JACC Basic Transl Sci* 2019;**4**:147–157. <https://doi.org/10.1016/j.jacpts.2018.12.005>
- Wittig I, Braun HP, Schagger H. Blue native PAGE. *Nat Protoc* 2006;**1**:418–428. <https://doi.org/10.1038/nprot.2006.62>
- Pereyra AS, Harris KL, Soepriatna AH, Waterbury QA, Bharathi SS, Zhang Y, et al. Octanoate is differentially metabolized in liver and muscle and fails to rescue cardiomyopathy in CPT2 deficiency. *J Lipid Res* 2021;**62**:100069. <https://doi.org/10.1016/j.jlr.2021.100069>
- Gnaiger E. *Mitochondrial Pathways and Respiratory Control*. Innsbruck: Mitochondr Physiol Network; 2007. 80.
- Nijenkamp L, Bollen IAE, van Velzen HG, Regan JA, van Slegtenhorst M, Niessen HWM, et al. Sex differences at the time of myectomy in hypertrophic cardiomyopathy. *Circ Heart Fail* 2018;**11**:e004133. <https://doi.org/10.1161/CIRCHEARTFAILURE.117.004133>
- Lang RM, Bierig M, Devereux RB, Flachskampf FA, Foster E, Pellikka PA, et al. Recommendations for chamber quantification: a report from the American Society of Echocardiography's Guidelines and Standards Committee and the Chamber Quantification Writing Group, developed in conjunction with the European Association of Echocardiography, a branch of the European Society of Cardiology. *J Am Soc Echocardiogr* 2005;**18**:1440–1463.
- Nagueh SF, Smiseth OA, Appleton CP, Byrd BF III, Dokainish H, Edvardsen T, et al. Recommendations for the evaluation of left ventricular diastolic function by echocardiography: an update from the American Society of Echocardiography and the European Association of Cardiovascular Imaging. *Eur Heart J Cardiovasc Imaging* 2016;**17**:1321–1360. <https://doi.org/10.1093/ehjci/ew082>
- Gottlieb RA, Bernstein D. Mitochondrial remodeling: rearranging, recycling, and reprogramming. *Cell Calcium* 2016;**60**:88–101. <https://doi.org/10.1016/j.ceca.2016.04.006>
- Ikon N, Ryan RO. Cardiolipin and mitochondrial cristae organization. *Biochim Biophys Acta Biomembr* 2017;**1859**:1156–1163. <https://doi.org/10.1016/j.bbmem.2017.03.013>
- Friedman JR, Mourier A, Yamada J, McCaffery JM, Nunnari J. MICOS coordinates with respiratory complexes and lipids to establish mitochondrial inner membrane architecture. *Elife* 2015;**4**:e07739. <https://doi.org/10.7554/eLife.07739>
- Shen J, Zhang JH, Xiao H, Wu JM, He KM, Lv ZZ, et al. Mitochondria are transported along microtubules in membrane nanotubes to rescue distressed cardiomyocytes from apoptosis. *Cell Death Dis* 2018;**9**:81. <https://doi.org/10.1038/s41419-017-0145-x>
- Xu Z, Schaedel L, Portran D, Aguilar A, Gaillard J, Marinkovich MP, et al. Microtubules acquire resistance from mechanical breakage through intraluminal acetylation. *Science* 2017;**356**:328–332. <https://doi.org/10.1126/science.aai8764>
- Chen J, Kholina E, Szyk A, Fedorov VA, Kovalenko I, Gudimchuk N, et al. Alpha-tubulin tail modifications regulate microtubule stability through selective effector recruitment, not changes in intrinsic polymer dynamics. *Dev Cell* 2021;**56**:2016–2028.e4. <https://doi.org/10.1016/j.devcel.2021.05.005>
- Dorsch LM, Schuldt M, dos Remedios CG, Schinkel AFL, de Jong PL, Michels M, et al. Protein quality control activation and microtubule remodeling in hypertrophic cardiomyopathy. *Cells* 2019;**8**:741. <https://doi.org/10.3390/cells8070741>
- Hershberger KA, Martin AS, Hirschey MD. Role of NAD(+) and mitochondrial sirtuins in cardiac and renal diseases. *Nat Rev Nephrol* 2017;**13**:213–225. <https://doi.org/10.1038/nrneph.2017.5>
- Wijnter PJM, Sequeira V, Kuster DWD, Velden JV. Hypertrophic cardiomyopathy: a vicious cycle triggered by sarcomere mutations and secondary disease hits. *Antioxid Redox Signal* 2019;**31**:318–358. <https://doi.org/10.1089/ars.2017.7236>
- Coats CJ, Heywood WE, Virasami A, Ashrafi N, Syrris P, Dos Remedios C, et al. Proteomic analysis of the myocardium in hypertrophic obstructive cardiomyopathy. *Circ Genom Precis Med* 2018;**11**:e001974. <https://doi.org/10.1161/CIRCGENETICS.117.001974>
- Ho CY, Day SM, Ashley EA, Michels M, Pereira AC, Jacoby D, et al. Genotype and lifetime burden of disease in hypertrophic cardiomyopathy: insights from the Sarcomeric Human Cardiomyopathy Registry (SHaRe). *Circulation* 2018;**138**:1387–1398. <https://doi.org/10.1161/CIRCULATIONAHA.117.033200>



42. Robertson J, Schaufelberger M, Lindgren M, Adiels M, Schioler L, Toren K, et al. Higher body mass index in adolescence predicts cardiomyopathy risk in midlife. *Circulation* 2019;**140**:117–125. <https://doi.org/10.1161/CIRCULATIONAHA.118.039132>
43. Fumagalli C, Maurizi N, Day SM, Ashley EA, Michels M, Colan SD, et al. Association of obesity with adverse long-term outcomes in hypertrophic cardiomyopathy. *JAMA Cardiol* 2020;**5**:65–72. <https://doi.org/10.1001/jamacardio.2019.4268>
44. Nollet EE, Westenbrink BD, de Boer RA, Kuster DWD, van der Velden J. Unraveling the genotype-phenotype relationship in hypertrophic cardiomyopathy: obesity-related cardiac defects as a major disease modifier. *J Am Heart Assoc* 2020;**9**:e018641. <https://doi.org/10.1161/JAHA.120.018641>
45. Ventura-Clapier R, Moulin M, Piquereau J, Lemaire C, Mericskay M, Veksler V, et al. Mitochondria: a central target for sex differences in pathologies. *Clin Sci* 2017;**131**:803–822. <https://doi.org/10.1042/CS20160485>
46. El-Hattab AW, Scaglia F. Mitochondrial cardiomyopathies. *Front Cardiovasc Med* 2016;**3**:25. <https://doi.org/10.3389/fcvm.2016.00025>
47. Kolwicz SC Jr, Purohit S, Tian R. Cardiac metabolism and its interactions with contraction, growth, and survival of cardiomyocytes. *Circ Res* 2013;**113**:603–616. <https://doi.org/10.1161/CIRCRESAHA.113.302095>
48. Wust RC, Helmes M, Stienen GJ. Rapid changes in NADH and flavin autofluorescence in rat cardiac trabeculae reveal large mitochondrial complex II reserve capacity. *J Physiol* 2015;**593**:1829–1840. <https://doi.org/10.1113/jphysiol.2014.286153>
49. Unno K, Isobe S, Izawa H, Cheng XW, Kobayashi M, Hirashiki A, et al. Relation of functional and morphological changes in mitochondria to myocardial contractile and relaxation reserves in asymptomatic to mildly symptomatic patients with hypertrophic cardiomyopathy. *Eur Heart J* 2009;**30**:1853–1862. <https://doi.org/10.1093/eurheartj/ehp184>
50. Ahmed MI, Guichard JL, Soorappan RN, Ahmad S, Mariappan N, Litovsky S, et al. Disruption of desmin-mitochondrial architecture in patients with regurgitant mitral valves and preserved ventricular function. *J Thorac Cardiovasc Surg* 2016;**152**:1059–1070 e2. <https://doi.org/10.1016/j.jtcvs.2016.06.017>
51. Gomez-Arroyo J, Mizuno S, Szczepanek K, Van Tassel B, Natarajan R, dos Remedios CG, et al. Metabolic gene remodeling and mitochondrial dysfunction in failing right ventricular hypertrophy secondary to pulmonary arterial hypertension. *Circ Heart Fail* 2013;**6**:136–144. <https://doi.org/10.1161/CIRCHEARTFAILURE.111.966127>
52. Shults NV, Kanovka SS, Ten Eyck JE, Rybka V, Suzuki YJ. Ultrastructural changes of the right ventricular myocytes in pulmonary arterial hypertension. *J Am Heart Assoc* 2019;**8**:e011227. <https://doi.org/10.1161/JAHA.118.011227>
53. Chaanine AH, Gordon RE, Kohlbrenner E, Benard L, Jeong D, Hajjar RJ. Potential role of BNP13 in cardiac remodeling, myocardial stiffness, and endoplasmic reticulum: mitochondrial calcium homeostasis in diastolic and systolic heart failure. *Circ Heart Fail* 2013;**6**:572–583. <https://doi.org/10.1161/CIRCHEARTFAILURE.112.000200>
54. Goh KY, Qu J, Hong H, Liu T, Dell'Italia LJ, Wu Y, et al. Impaired mitochondrial network excitability in failing guinea-pig cardiomyocytes. *Cardiovasc Res* 2016;**109**:79–89. <https://doi.org/10.1093/cvr/cvv230>
55. Guichard JL, Rogowski M, Agnetti G, Fu L, Powell P, Wei CC, et al. Desmin loss and mitochondrial damage precede left ventricular systolic failure in volume overload heart failure. *Am J Physiol Heart Circ Physiol* 2017;**313**:H32–H45. <https://doi.org/10.1152/ajpheart.00027.2017>
56. Pinali C, Bennett H, Davenport JB, Trafford AW, Kitmitto A. Three-dimensional reconstruction of cardiac sarcoplasmic reticulum reveals a continuous network linking transverse-tubules: this organization is perturbed in heart failure. *Circ Res* 2013;**113**:1219–1230. <https://doi.org/10.1161/CIRCRESAHA.113.301348>
57. Rajab BS, Kassab S, Stonall CD, Daghistani H, Gibbons S, Mamas M, et al. Differential remodelling of mitochondrial subpopulations and mitochondrial dysfunction are a feature of early stage diabetes. *Sci Rep* 2022;**12**:978. <https://doi.org/10.1038/s41598-022-04929-1>
58. Wilding JR, Joubert F, de Araujo C, Fortin D, Novotova M, Veksler V, et al. Altered energy transfer from mitochondria to sarcoplasmic reticulum after cytoarchitectural perturbations in mice hearts. *J Physiol* 2006;**575**:191–200. <https://doi.org/10.1113/jphysiol.2006.114116>
59. Ramaccini D, Montoya-Urbe V, Aan FJ, Modesti L, Potes Y, Wieckowski MR, et al. Mitochondrial function and dysfunction in dilated cardiomyopathy. *Front Cell Dev Biol* 2020;**8**:624216. <https://doi.org/10.3389/fcell.2020.624216>
60. Li J, Zhang D, Brundel B, Wiersma M. Imbalance of ER and mitochondria interactions: prelude to cardiac ageing and disease? *Cells* 2019;**8**:1617. <https://doi.org/10.3390/cells8121617>
61. Maack C, O'Rourke B. Excitation-contraction coupling and mitochondrial energetics. *Basic Res Cardiol* 2007;**102**:369–392. <https://doi.org/10.1007/s00395-007-0666-z>
62. Aon MA, Cortassa S, Marban E, O'Rourke B. Synchronized whole cell oscillations in mitochondrial metabolism triggered by a local release of reactive oxygen species in cardiac myocytes. *J Biol Chem* 2003;**278**:44735–44744. <https://doi.org/10.1074/jbc.M302673200>
63. Burgoyne JR, Mongue-Din H, Eaton P, Shah AM. Redox signaling in cardiac physiology and pathology. *Circ Res* 2012;**111**:1091–1106. <https://doi.org/10.1161/CIRCRESAHA.111.255216>
64. Maack C. Orphaned mitochondria in heart failure. *Cardiovasc Res* 2016;**109**:6–8. <https://doi.org/10.1093/cvr/cvv262>
65. Luongo TS, Eller JM, Lu M-J, Niere M, Raith F, Perry C, et al. SLC25A51 is a mammalian mitochondrial NAD(+) transporter. *Nature* 2020;**588**:174–179. <https://doi.org/10.1038/s41586-020-2741-7>
66. Zapata-Perez R, Tammara A, Schomakers BV, Scantlebury AML, Denis S, Elfrink HL, et al. Reduced nicotinamide mononucleotide is a new and potent NAD(+) precursor in mammalian cells and mice. *FASEB J* 2021;**35**:e21456. <https://doi.org/10.1096/fj.202001826R>
67. Connell NJ, Houtkooper RH, Schrauwen P. NAD(+) metabolism as a target for metabolic health: have we found the silver bullet? *Diabetologia* 2019;**62**:888–899. <https://doi.org/10.1007/s00125-019-4831-3>
68. Schwemmler J, Maack C, Bertero E. Mitochondria as therapeutic targets in heart failure. *Curr Heart Fail Rep* 2022;**19**:27–37. <https://doi.org/10.1007/s11897-022-00539-0>
69. Jussupow A, Di Luca A, Kaila VRI. How cardiolipin modulates the dynamics of respiratory complex I. *Sci Adv* 2019;**5**:eaav1850. <https://doi.org/10.1126/sciadv.aav1850>
70. Dai DF, Hsieh EJ, Chen T, Menendez LG, Basisty NB, Tsai L, et al. Global proteomics and pathway analysis of pressure-overload-induced heart failure and its attenuation by mitochondrial-targeted peptides. *Circ Heart Fail* 2013;**6**:1067–1076. <https://doi.org/10.1161/CIRCHEARTFAILURE.113.000406>
71. Sabbah HN, Gupta RC, Kohli S, Wang M, Hachem S, Zhang K. Chronic therapy with elamipretide (MTP-131), a novel mitochondria-targeting peptide, improves left ventricular and mitochondrial function in dogs with advanced heart failure. *Circ Heart Fail* 2016;**9**:e002206. <https://doi.org/10.1161/CIRCHEARTFAILURE.115.002206>
72. Olivetto I, Oreziak A, Barriaes-Villa R, Abraham TP, Masri A, Garcia-Pavia P, et al. Mavacamten for treatment of symptomatic obstructive hypertrophic cardiomyopathy (EXPLORER-HCM): a randomised, double-blind, placebo-controlled, phase 3 trial. *Lancet* 2020;**396**:759–769. [https://doi.org/10.1016/S0140-6736\(20\)31792-X](https://doi.org/10.1016/S0140-6736(20)31792-X)